High Throughput Screening Tools to Probe and Inhibit Core Fucosylation

Maxim Soroko

A Thesis

in

The Department

of

Chemistry and Biochemistry

Presented in Partial Fulfillment of the Requirements

for the Degree of Master of Science (Chemistry) at

Concordia University

Montreal, Quebec, Canada

Feb 2021

CONCORDIA UNIVERSITY

School of Graduate Studies

This is to certify that the thesis prepared

By: Maxim Soroko

Entitled: High Throughput Screening Tools to Probe and Inhibit Core Fucosylation

and submitted in partial fulfillment of the requirements for the degree of

Master of Science (Chemistry)

complies with the regulations of the University and meets the accepted standards with respect to originality and quality.

Signed by the final Examining Committee:

_____ Chair

Paul Joyce

_____ Examiner

Brandon Findlay

_____ Examiner

Pat Forgione

_____ Supervisor

David Kwan

Approved by _____ Graduate Program Director

Yves Gelinas

_____ _____ Dean of Faculty

Date *Pascale Sicotte*

Abstract

High Throughput Screening Tools to Probe and Inhibit Core Fucosylation

Maxim Soroko

We report a chemo-enzymatic transglycosylation synthesis of the 4-methylumbelliferyl glycoside of a complex-type oligosaccharide substrate for core fucosylation. We demonstrate the use of the glycoconjugate in a newly developed enzyme assay to probe the activity and inhibition of fucosyltransferase VIII, which catalyzes the core fucosylation of *N*-glycans found on eukaryotic glycoproteins. In our assay, the fucosyltransferase VIII reaction is coupled to a specific glycosidase enzyme, allowing to distinguish an unmodified 4-methylumbelliferyl oligosaccharide probe from the fucosylated probe. Our results demonstrate that the assay is very sensitive and specific to the detection of enzymatic activity, while also enabling the identification of potential fucosyltransferase VIII inhibitors.

Acknowledgements

This work was financially supported by a Discovery Grant (grant no. RGPIN-2016-05464) from the Natural Sciences and Engineering Research Council of Canada, an Individual Seed Funding Program Grant from Concordia University, and a Petro-Canada Young Innovator Award Grant to D.H.K. I thank Concordia University for a scholarship support through a Campaign for Concordia Graduate Award. I also thank Marcos di Falco for his support in performing HPLC-MS analysis and Kathy Mu and Haoyu Wu for their assistance in preparing recombinant enzymes. Several of the plasmids used to express recombinant proteins were the kind gift of Stephen Withers, and recombinant human FUT8 was the kind gift of Kenta Yamato, Jae Man Lee, and Takahiro Kusakabe. I am grateful to Pat Forgione, Christopher J. Wilds, Lai-Xi Wang, Stephen Withers, and David Vocadlo for helpful discussions in the course of this work.

Contribution Statement

This work was performed jointly by David H. Kwan and Maxim Soroko. Text for sections 1.1, 2.1, and 3.3 were modified from a publication submitted by David H. Kwan and Maxim Soroko. The remaining sections in this work were written by Maxim Soroko and reviewed by David H. Kwan. Data for figures 3.13 and 3.14 were generated by David H. Kwan in repeat experiments initially performed by Maxim Soroko. The remaining data reported in this work was generated by Maxim Soroko. Figures 3.13, 3.14 and 3.15 were designed by David H. Kwan with the remainder of the figures designed by Maxim Soroko.

Table of Contents

Chapter Three

Results and discussion

Chapter Four

Conclusion

List of figures

List of Abbreviations

ACN: Acetonitrile

ADCC: Antibody-dependent cellular cytotoxicity

ATP: Adenosine-5'-triphosphate

BgaA: Exo-β-galactosidase from *Streptococcus pneumoniae*

DMC: 2-chloro-1,3-dimethylimidazolinium chloride

DMSO: Dimethyl sulfoxide

EGF: Epidermal growth factor

EGFR: epidermal growth factor receptors

EMT: epithelial-mesenchymal transition

EndoM: Endo-β-*N*-acetylglucosaminidase from *Mucor hiemalis*

EndoM N175Q: Endo-β-*N*-acetylglucosaminidase N175Q from *Mucor hiemalis*

FKP: L-fucokinase/GDP-fucose pyrophosphorylase from *Bacteroides fragilis* 9343

Fuc: Fucose

FUT: Fucosyltransferase

FUT8: Human α-(1,6)-fucosyltransferase

G0: complex-type asialo-, agalacto-, biantennary heptasaccharide

G0F: Fucosylated complex-type asialo-, agalacto-, biantennary heptasaccharide

Gal: Galactose

GalNAc: *N*-acetylgalactosamine

GBP: Glycan-binding proteins

GDP: Guanosine-5'-diphosphate

GDP-Fucose: guanosine 5′-diphospho-β-L-fucose

GDP-2F-Fuc: Guanosine-5′-diphospho-2-deoxy-2-fluoro-β-L-fucose

GlcNAc: *N*-acetylglucosamine

GTP: Guanosine-5'-triphosphate

HPLC-MS: High performance liquid chromatography – mass spectrometry

IPTG: Isopropyl β-D-1-thiogalactopyranoside

Man: Mannose

MET: Mesenchymal-Epithelial transition

MS: Mass Spectrometry

MU: 4-methylumbelliferone

MU-G0: 4-methylumbelliferyl glycoside of the G0 heptasaccharide

MU-G0F: Fucosylated 4-methylumbelliferyl glycoside of the G0 heptasaccharide

MU-G2S2: 4-methylumbelliferyl glycoside of the G2S2 complex-type glycan

MU-GLCNAC: 4-methylumbelliferyl β-*N*-acetylglucosamine

NanH: exo-α-neuraminidase from *Clostridium perfringens*

PNGaseF: Peptide *N*-glycosidase F from *Flavobacterium meningosepticum*

SGP: Sialoglycopeptide

sLeX: Sialyl-Lewis X

SpHex: exo-β-*N*-acetylhexosaminidase from *Streptomyces plicatus*

TFA: Trifluoroacetic acid

TGF-β: Transforming growth factor beta

TLC: Thin layer chromatography

VEGFR: vascular endothelial growth factor receptor

1 Introduction

1.1 Glycobiology introduction

Glycobiology—the study of the structures, functions, and biology of glycans (also known as carbohydrates, saccharides, or sugars)—has been a field mostly unexplored. Thanks to the recent technological developments, researchers are now able to delve deeper into the field. Glycans are believed to be the most complex biological molecules found in nature (1) due to the sheer number of existing molecules, as one database reports more than 700 existing monosaccharide building blocks across all living organisms (2). Fortunately, the human glycome (the entirety of carbohydrates in a cell) is much less daunting; consisting primarily of only nine monosaccharide building blocks, most of which are structurally similar and often vary from one another by a single carbon configuration (3). These nine building blocks are D-glucose, *N*-acetyl-D-glucosamine, D-galactose, *N*-acetyl-D-galactosamine, D-mannose, D-xylose, D-Glucuronic acid, L-Fucose and *N*-acetylneuraminic acid **(Figure 1.1)**. In contrast to amino acids in proteins or nucleotides in nucleic acids which are assembled in a linear sequence, glycans are assembled in a branched-like sequence. Monosaccharides units are linked to one another in one of two possible stereochemical configurations (α and β), usually from the anomeric center of one monosaccharide to any of the three or four hydroxyl groups of the other monosaccharide, but there are also scenarios where the anomeric center is not involved, and units are linked through the other hydroxyl groups. These different structural possibilities are what gives rise to the great glycan diversity. To better illustrate this diversity, three different monosaccharides can combine to make over 1000 structures while three different amino acids can combine to make only 6 distinct structures (4).

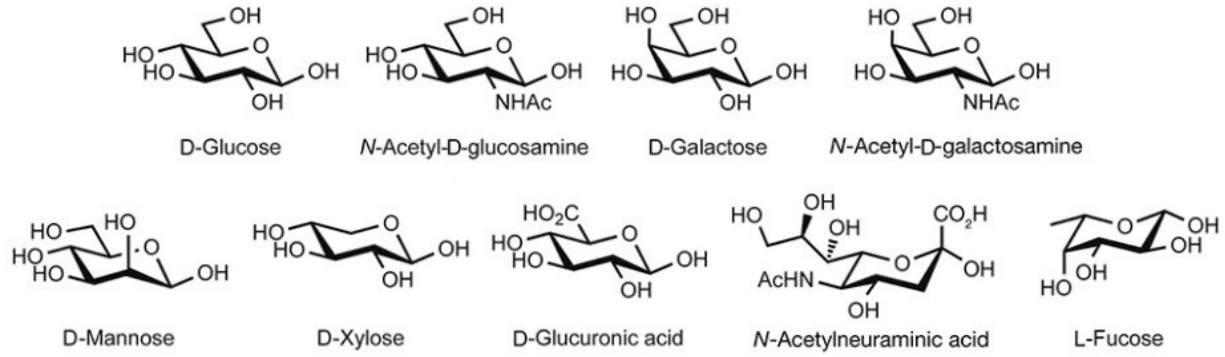

Figure 1.1. Common monosaccharides found in vertebrates.

Monosaccharides are assembled into complex glycan structures by glycosyltransferase enzymes, in a process known as glycosylation. These complex glycans are usually found on proteins or lipids, and they form the glycocalyx of every living eukaryotic or prokaryotic cell (5). Glycans are synthesized and secreted on proteins as either *N*-glycans (nitrogen linked) attached to asparagine residues on an Asn-X-Ser/Thr motif, or as *O*-glycans (oxygen linked) attached to serine or threonine residues (6) **(Figure 1.2)**. *N*-glycans possess a common core structure, consisting of three mannose and two acetylglucosamine residues ($Man_3GlcNAc_2Asn$). *N*-glycans are also classified into three different categories: oligomannose type which contain only mannose residues attached to the core structure; complex type which possess similar oligosaccharide sequences on both of their antenna; and hybrid types which have an oligomannose sequence on the 1,3 arm and a complex type-like sequence on the 1,6 arm (7). In contrast, *O*-glycans do not have a starting common core structure. Rather, they are classified into one of four different core structures that start with an *O*-GalNAc attached to the Ser/Thr residues and the cores can be either extended, branched or terminated with Fucose, Sialic acid or blood group antigens (8).

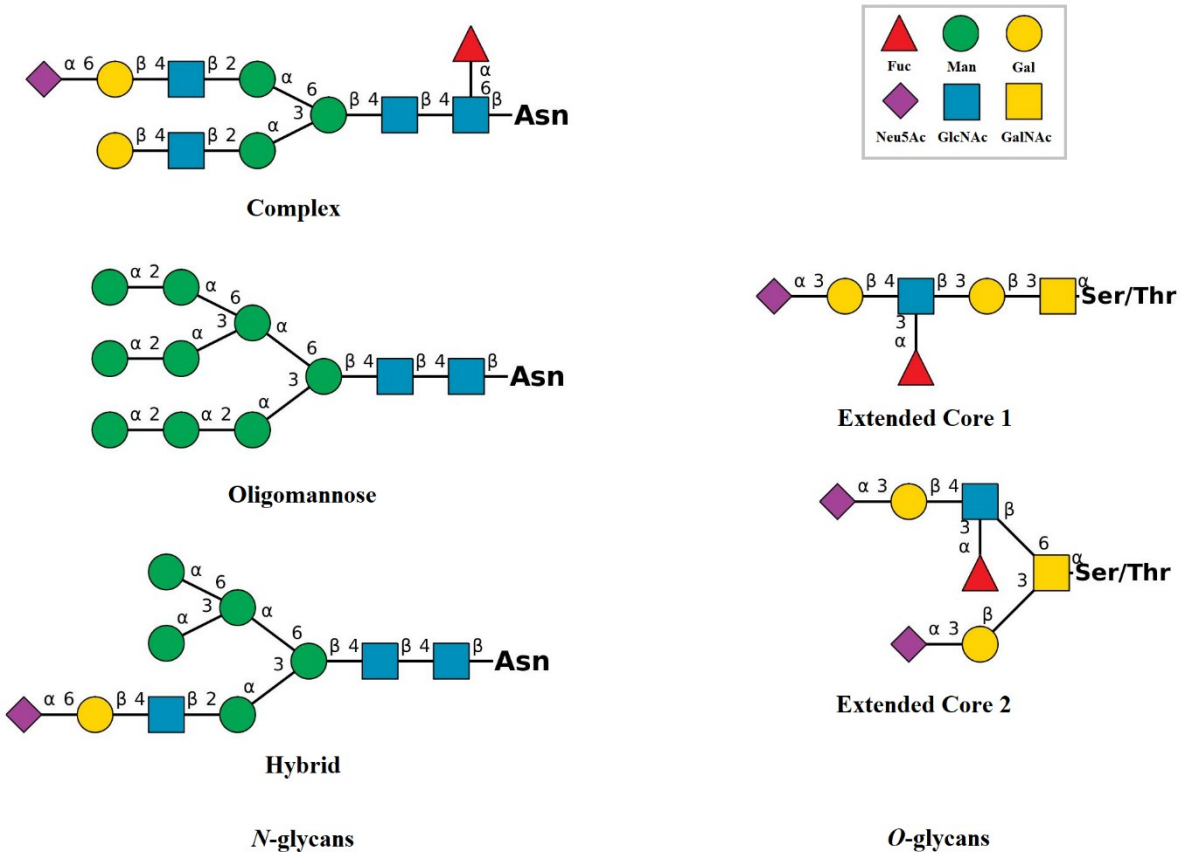

Figure 1.2. Examples of some types of N-glycans and O-glycans.

The synthesis of the glycans present on glycoproteins occurs as a post-translational modification in the endoplasmic reticulum or in the Golgi apparatus and aids in the proper folding and stabilization of nascent protein structures (9). Mature proteins are then transported to cell surface membranes, where their glycans can be recognized by specific molecules known as glycan-binding proteins (GBPs) (10). GBPs are complementary proteins because they each possess a carbohydrate recognition domain, capable of binding to a specific grouping of about two-to-seven monosaccharides in specific configurations (11). Through their interactions with GBPs, glycans participate in a vast number of biological functions which can be divided into four distinct categories (10): 1) structural and modulatory roles; 2) intrinsic recognition; 3) extrinsic recognition; and 4) molecular mimicries.

Structural and modulatory roles: glycans provide many protective, stabilizing, organizational, and barrier-like functions. For example, β-linked polymers of glucose or *N*-acetylglucosamine come together to form cellulose or chitin, respectively. These structures are

very difficult to break down by any physical, chemical, or enzymatic means as they possess a certain strength and rigidity that provides structural integrity and support to the cell walls of plants/fungi and arthropod exoskeletons (12, 13). Intrinsic (intraspecies) recognition: glycans participate in many specific biological roles in cell-cell recognition and cell-matrix interactions. For example, glycan-recognition processes are involved in several steps of sperm-egg interactions during fertilization and reproduction; these include migration of the sperm to the site of fertilization, destruction of sperm carrying nonspecies-specific antigens, implantation of the fertilized egg and placental development (14). The examples above are regulated and coordinated by the glycans found on cell surfaces and are not only limited to fertilization. Extrinsic (interspecies) recognition: this category concerns glycans involved in interactions between host cells and microbes. Pathogens and symbionts have evolved many mechanisms to better recognize specific structures of cell surface glycans in their target host species (15). For example, bacteria and viruses can recognize the sialic acid moieties at the non-reducing ends of complex glycans and use these sugars as the initial binding sites to their targets, and it is through the different sialic acid linkages that pathogens such as the influenza virus can differentiate human hosts from avian hosts (16). Finally, molecular mimicries: pathogens decorate themselves with glycans identical to those present on host cell surfaces. Since the host immune system can recognize typical glycans found on pathogens, microorganisms have evolved different mechanisms to better mimic the host's cell surface glycans and avoid detection by the immune system. These mechanisms range from acquisition of host sialoglycans (glycans with sialic acids at the non-reducing terminals) (17) to transfer of sialic acids from host to pathogen by the host's enzymes (18), to efficient uptake of free cellular sialic acids (19). In short, pathogens invade the host glycosylation machinery and avoid detection from the host's immune system.

1.2 Cell-surface carbohydrates

Complex glycans expressed on cellular glycoproteins and glycolipids are essential for proper development and cellular differentiation in higher organisms as these carbohydrates regulate cell adhesion, recognition and signaling (20). In this sense, glycans encode the information necessary to perform cellular processes. These processes are communicated by lectins (a type of GBPs) that specifically recognize the complex carbohydrate structures and transduce the

information into a cellular signaling event (21). There are several different types of lectins that exist in nature, we will describe a selected few example below.

1.2.1 Cell-surface carbohydrates – cell adhesion

Integrins are a family of GBPs involved in cell adhesion. Integrins interact with the extracellular matrix and function as signal-transducing receptors by activating different pathways for cell activation and proliferation (22). Previous studies have demonstrated how integrin activation is modulated by the presence of oligosaccharides. For example, when human fibroblasts were cultured with an inhibitor of alpha-mannosidase II (an enzyme that cleaves mannose residues from oligosaccharides), the fibroblasts displayed immature α5β1 integrin on their cell surfaces and fibronectin dependent adhesion was greatly reduced (23). The inhibitor was inactivating alpha-mannosidase II, thus preventing processing of N-glycans into their mature form during glycoprotein synthesis. Another study demonstrated treatment of purified α5β1 integrin with N-glycosidase F resulted in a blockage of α5β1 integrin adhesion to fibronectin since the N-linked oligosaccharides have been cleaved off from the asparagine residues due to N-glycosidase F (24). Lastly, increased sialylation (a form of glycosylation involving sialic acids) of the β1 subunit of α5β1 integrins correlated with decreased adhesiveness properties to fibronectin (25), whereas enzymatic removal of sialic acids from the α5 integrin subunit completely inhibited cell adhesion to fibronectin (26). Thus, these studies demonstrated the importance of N-glycosylation of integrin α5β1 in its interactions with fibronectin for cell adhesion.

1.2.2 Cell-surface carbohydrates – cell differentiation

Human epidermal growth factor receptors (EGFR) play key roles in cell growth and differentiation. The receptors are composed of an extracellular epidermal growth factor (EGF) binding domain, a transmembrane spanning portion, an intracellular protein-tyrosine kinase domain for signaling, and a carboxyl terminal tail (27). To exert its activity, human EGFR dimerizes upon binding of EGF ligands, thus activating the protein-tyrosine kinase and initiating a downstream signaling cascade (28). Human EGFR possesses 11 well-established *N*-glycosylation sites involved in modulating the receptor's activity (29). Previous studies revealed that elimination of *N*-linked oligosaccharides at the Asn420 position causes spontaneous dimerization of EGFR and a constitutively activated kinase domain even in absence of EGF (30).

The result is an uncontrollable activated receptor, leading to increased growth and proliferation. Through this example, we can see the importance that carbohydrates play in modulating the activity of receptors in cell growth and differentiation.

1.2.3 Cell-surface carbohydrates – immune system

There exist several functions for glycans in immunology, and by extension, GBPs are also implicated in the immune system. The different carbohydrate structures found on cell surfaces of host cells and pathogenic invaders constitute the basis of immune responses, including immune cell activation, trafficking, and regulation (31). For example, in response to inflammation, selectins are mobilized to the vascular endothelial cell surfaces facing the blood vessel lumen, where they bind to complementary glycans on the surface of passing neutrophils. Neutrophils will then roll on the endothelium lining until other cell mechanisms are triggered that allow neutrophil extravasation into infected tissues and combat the pathogenic invaders (32). This mechanism known as leukocyte rolling, is mediated by P-selectin (platelet) and E-selectin (endothelial). These two selectins are structurally similar and bind to closely related glycans on neutrophil surfaces (33). Their binding target is a tetrasaccharide structure called sialyl Lewis^X (sLe^x) with key recognition features being a sialic acid and a fucose residue (34). If the sLe^X antigen is not expressed, then selectins fail to bind to circulating leukocytes (35) and an immune response cannot be mediated. Thus, glycans are important for the immune system to respond to inflammation.

Surface-localized glycoproteins of the immune system are not the only proteins affected by glycans; secreted glycoproteins such as antibodies can also have their activity modulated by glycans. Antibodies are large, Y-shaped proteins consisting of three roughly equal-sized domains. The two arms of the Y are termed the Fab fragments and constitute the antigen-binding sites of the molecule, whereas the trunk of the Y, called the Fc fragment, is responsible for interacting with effector cells (cells that respond to a stimulus) (36). The Fc region is formed of two heavy polypeptide chains, each with a single N-glycan attached at Asn297 that is responsible for imparting the antibody conformation of the fragment via glycan-protein and glycan-glycan interactions (37). Humans have a total of six Fc receptors (FcγRI, FcγRIIa, FcγRIIb, FcγRIIc, FcγRIIIa and FcγRIIIb) all expressed at different levels on all innate immune cells and it is the shape of the Fc region that defines the capability of the antibody to interact with the Fc receptors

of effector cells (38). In fact, the Fc region of antibodies is heavily glycosylated and these glycans enable antibody-receptor binding - removal of glycans of the Fc region results in a complete loss of Fc receptor binding to the antibodies (39). One recent discovery showed that *N*-glycans on the Fc portion modulate antibody activity by sending inhibitory signals to responding immune cells if terminal sialic acids are present on the glycans, or by sending activating signals if terminal sialic acids are missing (40, 41). This discovery led to the use of glyco-engineered antibodies for therapeutic purposes (42), which will be further addressed later in the text. Taken together, these findings demonstrate the role and importance that glycans have on antibodies, and in the immune system.

1.2.4 Cell-surface carbohydrates – cancer

Knowing that glycans are prime targets of pathogenic invaders like microbes and viruses (15, 16), it is not surprising that they are also targets of different types of cancers. Most cancer related deaths are attributed to the metastatic spread of cancer cells to vital organs rather than due to the primary tumor growth. Malignant cells acquire characteristics that enable them to dissociate from the initial tumor site, degrade the extracellular matrix, invade into the blood stream, adhere onto secondary colonization sites, and metastasize (43, 44). These characteristics are acquired from the abnormal carbohydrates found on tumor cell-surfaces due to altered glycosylation (45), which then enable cancer cells to hijack the lectins expressed on endothelial cells, on immune cells or in the extracellular matrix to grow and proliferate at the host's detriment (46). Altered glycosylation arises from one of four contributing factors or a combination of some factors. The first is altered glycan expression from overexpression of glycosyltransferases. Enzymes that contribute to cancer metastasis are overexpressed in the tumor cell whereas enzymes that prevent cancer metastasis are repressed. These changes in expression levels can be caused either due to dysregulation of gene expression at the transcriptional level (47), dysregulation of chaperone function resulting in the synthesis of tumor-specific neo-epitopes (48), or altered glycosidase activity resulting in protection against programmed cell death (49). The second is altered glycan expression due to changes in the tertiary structure of proteins. Genomic mutations of associated glycosyltransferases could result in amino acid substitutions or changes in folding conformations, giving rise to new sites of glycosylation, or resulting in deletion of wild-type sites of glycosylation necessary for regulatory enzymatic activity (50). The third is the variety and abundance of sugar nucleotide donors. Tumor

cells rewire their metabolism to promote growth and proliferation by increasing uptake of various monosaccharides. This leads to an abundance of sugars in tumor cells that can be utilized for the synthesis of sugar nucleotide donors that will then participate in the synthesis of common tumor-cell epitopes (51). Lastly, the fourth is expression of relevant glycosyltransferases in the Golgi apparatus. The acidification of Golgi environment results in disorganization and fragmentation of the Golgi apparatus, and the acidic Golgi pH is critical for cancer-associated glycosylation and the expression of cancer-associated carbohydrate antigens (52). Taken together, these factors contribute to the expression of common tumor-cell epitopes such as sialyl Lewis^{X} and sialyl Lewis^{A} found in almost every type of cancer (45). For example, an increased expression of fucosyltransferase VII and α-2,3-sialyltransferase ST3Gal1—two enzymes involved in the synthesis of sialyl Lewis$^{X/A}$—has been observed (53). These glycans are critical for metastasis as they are the ligands of selectins found on endothelial blood vessel lining and allow cancer cells to adhere to secondary colonization sites.

An important function hijacked by cancer cells to facilitate metastasis is the epithelial-mesenchymal transition (EMT). The EMT is a biological process during which an epithelial cell undergoes multiple biochemical changes to transform into a mesenchymal cell with enhanced migratory capabilities (54). Epithelial tumor cells exploit EMT to acquire an invasive phenotype, facilitating their dissociation from the primary tumor and entering the blood circulation (55). This phenotype is gained by expressing the relevant glycans that participate in EMT. In short, cancer cells would overexpress enzymes that build the necessary glycans for EMT to occur and downregulate others that prevent altered glycosylation from happening. Furthermore, metastatic colonization at distant organs requires recovery of the epithelial characteristics, essentially reversing EMT in a process called mesenchymal-epithelial transition (MET) (56). It was only recently discovered that MET plays a role in cancer, and little is currently known compared to the extensive studies of EMT in tumor metastasis. This discovery sparked the hypothesis that tumor cells might exist in a partial-EMT state, changing between epithelial and mesenchymal phenotypes as needed (57). Thus, this example illustrates the importance of cell-surface carbohydrates in cancer metastasis.

1.3 Fucosylation - overview

The cellular processes described above are controlled by a biological process called fucosylation. Fucosylation is observed in vertebrates, invertebrates, plants, fungi, and bacteria, wherein the monosaccharide L-fucose is incorporated into complex glycans. These fucosylated carbohydrates are involved in a wide variety of biological functions including cell adhesion, cell development, angiogenesis, fertilization, immune response and activation, malignancy, and tumor metastasis (58, 59). Fucosylation is carried out by fucosyltransferase enzymes that catalyze the transfer of fucose residue from guanosine diphosphate fucose (GDP-Fuc) to acceptor molecules. There are thirteen fucosyltransferase enzymes identified in humans, which catalyze either α-(1,2)-, α-(1,3/4)-, α-(1,6)- or *O*- fucosylations (60). *O*-fucosylation is an *O*-linked glycosylation that occurs on serine and threonine residues of glycoproteins, whereas the others are *N*-linked glycosylations that can be divided into two categories: core fucosylation catalyzed by α-(1,6)-FUTs that occur on the innermost moieties of *N*-glycans, and terminal fucosylation catalyzed by α-(1,2)- and α-(1,3/4)- FUTs at the non-reducing ends (60).

1.3.1 Fucosylation – terminal fucosylation

Ten fucosyltransferases (FUT1-7 and FUT9-11) are responsible for carrying out the addition of fucose residues for terminal fucosylation to generate sialyl-Lewis antigens. These antigens are the ligands of selectins expressed on glycoproteins and glycolipids involved in leukocyte adhesion, migration, and trafficking of the E-, P- and L- selectins mentioned previously (61). Sialyl antigens also play a role in facilitating cancer metastasis as a byproduct of their natural role in promoting selectin-mediated rolling and adhesion of white blood cells to endothelial tissue linings (62). These antigens are upregulated in several malignant cancers such as lung, breast and colorectal cancers and are usually indicators of poor prognosis (63). For example, studies have shown that elimination of fucose residues from sialyl antigens impairs the ability of cancer cells to roll on the endothelial lining (64), whereas elimination of terminal fucosylation by knocking down certain *FUT* genes inhibits tumor growth altogether (65).

1.3.2 Fucosylation – core fucosylation

In contrast to terminal fucosylation, core fucosylation is the more commonly occurring type of fucose modification and is exclusively catalyzed by FUT8. Core fucosylation plays essential roles in normal physiological developments. For example, knocking out FUT8 in mice significantly decreases postnatal survival, with 70% of mice dying within three days of age, whereas the remaining 30% display severe growth retardation (66). FUT8-null mice also exhibit multiple abnormal behaviors associated with schizophrenia, such as increased locomotion (67). These phenotypes are due to the lack of core fucose, resulting in abnormal lung development and a decreased regulation of the TGF-β1 signaling pathway (66).

Wang *et al.* (68) were the first to investigate the effect of core fucosylation of *N*-glycans on the binding of EGF to its receptor. The authors reported a down-regulation of EGF-induced phosphorylation of EGFR in FUT8-null cells, resulting in a decreased EGFR-mediated downstream signaling (which controls biological responses such as proliferation, differentiation, cell motility and survival). However, these FUT8-null cells were rescued upon the reintroduction of the *Fut8* gene. Furthermore, the authors uncovered that there exist two classes of EGFR, a high binding affinity class and a low binding affinity class. Both classes are detectable in FUT8 wild type cells and restored cells, but only the low binding affinity class is detectable in FUT8-null cells. The authors postulated that core fucosylation is only required for the high binding affinity class, but further studies are necessary to elucidate the exact mechanism involved.

Similarly, Zhao *et al.* (69) reported that core fucosylation also plays an essential role in α3β1 integrin functions because cells deficient in core fucosylation displayed a blockage in α3β1 integrin-mediated cell migration and cell signaling. Once again, reintroduction of the *Fut8* gene into FUT8-null cells partly rescued the cells. These results correlated with their observations that purified α3β1 integrin possessed several bi-, tri-, and tetra-antennary complex type glycans that were mostly core fucosylated. Integrins and growth factor receptors share several elements in their signaling pathways, which could explain why core fucosylation is essential for integrins, but the molecular mechanisms remain to be elucidated.

Core fucosylation is also important in regulating the immune system, specifically in modulating antibody-dependent cellular cytotoxicity (ADCC) (70), a mechanism of immune defense where an effector cell lyses a target cell that displays surface antigens for the antibody to

bind. As was described previously, antibodies are Y-shaped molecules composed of two antigen-binding sites (the arms of the Y) and an Fc region (the stem of the Y). The Fc region of antibodies is heavily fucosylated with two *N*-linked biantennary complex-type oligosaccharides bound to an asparagine residue at position 297 (70). These oligosaccharides possess a core fucose residue that can influence the binding affinity of the effector cell receptor (FcγRIIIa) to the antibody's Fc region. Previous studies have demonstrated that removal of the core fucose from the Fc region oligosaccharides can greatly enhance the effector cell's ADCC potency (71, 72). Co-crystal structure analysis revealed that the receptor is incapable of high affinity binding when the core fucose is present because the core fucose causes a steric clash which weakens carbohydrate-carbohydrate interactions with neighboring oligosaccharides (73). When the core fucose is removed from the oligosaccharide at Asn297, a small conformational change takes place that allows the neighboring Tyr296 to hydrogen bond with its environment in a way that it previously was not capable of doing due to the core fucose hydrogen bonding in the Tyr296 environment (74). This small conformational change allows for ADCC potency to be enhanced from by 50- to 100-fold (75).

Fucosylated glycans on certain glycoproteins also serve as important cancer biomarkers (76). For example, elevated levels of α-fetoprotein (a fetal analog of serum albumin with fucosylated carbohydrate moieties) are used as a reliable biomarker for hepatocellular carcinoma (liver cancer) (77); core fucosylated haptoglobin has been identified as a biomarker for detecting pancreatic cancer which previously lacked reliable methods of early detection (78); in patients with prostate cancer, core fucosylation of prostate-specific antigen is another reliable marker that allows for the differentiation of prostate cancer from diseases like benign prostate hyperplasia that also affect prostate-specific antigens (79). These are just some examples to illustrate how frequent core fucosylation is hijacked by malignant cancers. In fact, several studies (80) have reported that silencing core fucosylation in cancer cells that express high levels of FUT8 resulted in the inhibition of cell invasion (81), cell migration (82), proliferation (83), colony formation (84), tumor growth and metastasis (85). The specific molecular mechanisms by which core fucosylation is involved in all these biological processes is through the regulation of important growth factor signaling pathways such as TGFβ (85), EGFR (86), and VEGFR (87), as well as impacting the

activity of membrane proteins involved in cell adhesion such as integrins (88) and E-cadherins (89).

These signaling pathways and membrane proteins are all implicated in the epithelial-mesenchymal transition (EMT), a process hijacked by cancer cells to dissociate from their primary tumor site, circulate in the blood stream and colonize secondary distal tumor sites. Tu *et al.* (85) identified a novel mechanism for breast cancer EMT triggered by TGFβ signaling. They observed that FUT8 is upregulated during TGFβ-induced EMT in breast carcinoma cells which lead to a remodeling of the *N*-glycans on cell surface receptors TGFβ RI and RII, resulting in enhanced ligand binding and increased downstream signaling activity. These remodeling events facilitated the transformation of epithelial cancer cells into mesenchymal cancer cells with increased migratory and invasive capabilities, allowing for distal lung metastasis. However, pharmacological inhibition or gene knock-down of FUT8 was sufficient to interrupt FUT8-promoted TGFβ signaling and suppressed the mobility, invasiveness, and lung metastasis of breast carcinoma cells both *in vitro* and *in vivo*. Further studies exploring the structural and functional effects of TGFβ receptors during EMT after being core fucosylated could shed light on the precise molecular mechanisms involved.

1.3.2.1 Core Fucosylation – anti-cancer treatments

Core fucosylation effects many biological functions of glycoproteins but the molecular mechanisms remain to be elucidated. Insights into the downstream effects of core fucosylation could be aided by using specific small molecule inhibitors that influence the activity of FUT8. These small molecule inhibitors can be used either as chemotherapeutic agents in the treatment of malignant cancers or in the production of therapeutic glycoproteins for cancer immunotherapy. It was reported that FUT8 is upregulated up to four times more in metastatic cancers than it is expressed in normal healthy cells (85). This difference in expression levels can provide a therapeutic window to combat cancer metastasis. At the right concentration of chemotherapeutic agent, FUT8 expression in cancer cells may be greatly hindered while FUT8 expression in healthy cells is only minimally affected. This would hopefully prevent the severe propagation of metastatic cancers in a host and allow for a tighter control over the disease's development.

Similarly, afucosylated monoclonal antibodies can be produced to selectively and efficiently kill cancer cells through ADCC, because monoclonal antibodies lacking core fucose bind more tightly to the FcγRIIIA receptors on natural killer cells than do their core-fucosylated counterparts (72, 90). In fact, the discovery that ADCC can be enhanced by inhibiting core fucosylation sparked the development of monoclonal antibodies to be used for therapeutic purposes by several pharmaceutical companies (91). For example, two afucosylated mAbs have been approved by the FDA for use in cancer patients, mogamulizumab which targets a signal transducer upregulated in leukemia and lymphoma (92), and obinutuzumab which is used in the treatment of chronic lymphocytic leukemia (93). Most *in vivo* studies on the effect of enhanced ADCC activities by afucosylated antibodies have been performed using genetic manipulation techniques to generate the glycoengineered antibodies (94). While genetic manipulation is certainly efficient, production of afucosylated antibodies by pharmacological inhibition of core fucosylation may also be of interest to the scientific community. One advantage of pharmacological inhibition (among others) is that the protein function is merely blocked and the protein remains in the cell, whereas in genetic manipulation the protein is completely removed; this may shed light on some mechanisms of ADCC enhancement because the protein can still interact with binding partners.

Thus, the development of small molecule inhibitors for core fucosylation can be of great interest to the scientific community, however developing such inhibitors remains a challenge (95). To better understand how to design FUT8 inhibitors, it is worthwhile to investigate the protein structure and function of the enzyme. FUT8 catalyzes the transfer of a fucose residue from GDP-Fucose donors to the innermost *N*-acetylglucosamine residue of acceptor *N*-glycans substrates by forming an α-1,6-linkage with inversion of the anomeric carbon center of the transferred fucose residue (96). FUT8 is abundant in brain tissue (97) and was originally isolated from porcine brain (98) and human gastric cancer cells (99).

FUT8 was reported as a type II transmembrane protein localized in the Golgi apparatus (99). The crystal structure of FUT8 in its unbound form was determined at 2.6 A resolution (100). The structure consists of three domains: an *N*-terminal coiled-coil domain, a catalytic domain and a C-terminal SH3 domain, a characteristic beta-barrel conformation consisting of six β-strands (100). The catalytic region is closely similar to GT-B glycosyltransferases with the C-terminus

end of the catalytic domain including a Rossman fold essential for enzymatic activity and consisting of three regions that are conserved among α-1,6-, α-1,2- and *O*-fucosyltransferase proteins (100). FUT8 requires the presence of the nitrogenous base portion and the diphosphoryl group of GDP to recognize the donor substrate molecule (101). The enzyme's specificity towards acceptor substrates is rather unusual as it recognizes an *N*-glycan with a tri-mannose core containing a β-1,2-acetylglucosamine residue linked to the α-1,3-mannose arm (102) but the presence of a bisecting acetylglucosamine in the tri-mannose core or an α-1,3-linked fucose to the innermost acetylglucosamine at the reducing end (103) can prevent the enzymatic reaction. Lastly, the glycosidic linkage between the acetylglucosamine moiety at the reducing end and the asparagine residue of the peptide consensus sequence appears to not be necessary for the enzymatic reaction (104). Based on the docking model of FUT8 in complex with the GDP-Fucose donor and oligosaccharide acceptor substrate, FUT8 was proposed to perform a S_N2 mechanism with base-catalyzed deprotonation of the acceptor substrate, in which Arg365 plays crucial roles in binding and stabilizing the GDP-Fucose donor (105). While the catalytic domain has been studied and described, the physiological functions of the other two accessory domains remains unclear.

1.4 Hypothesis and research project

Complex glycans attached to cell surface proteins play essential roles in biological processes, making them important structures to study. However, the lack of tools and the inherent complexity of glycans proved to be major roadblocks in studying glycobiology. It is only due to recent technological advances that enabled researchers to study glycans in biology (106). Core fucosylation is no exception – much is still unknown about its mechanisms and functionalities. The current tools available to monitor FUT8's activity are designed to detect nucleotide by-products released from coupled reaction, rather than detecting the oligosaccharide products generated from the FUT8-catalyzed reaction.

For this reason, we developed a strategy to efficiently assay the activity and inhibition of FUT8 in a high throughput manner. Our approach was built upon a previously developed method that detects the activity and inhibition of glycosyltransferases (107). The previous method in question is a fluorescence-based assay that uses a fluorogenically labeled oligosaccharide probe coupled with a specific glycosidase enzyme to distinguish unmodified probes from those modified

by a glycosyltransferase. As such, we have synthesized a 4-methylumbelliferyl oligosaccharide, MU-G0, as a substrate and fluorogenic probe for FUT8 by chemo-enzymatic synthesis. The probe can also be recognized by a chitinase enzyme, which will release the fluorophore, 4-methylumbelliferone, from the oligosaccharide, producing a fluorescent signal. However, if the fluorogenic probe is first treated with FUT8 and becomes fucosylated, the chitinase will no longer be able to digest the fucosylated-fluorogenic probe and no fluorescent signal will be detectable. Using this method, we can measure the activity of FUT8 using only picomole concentrations of probe and enzyme.

2 Materials and Methods

2.1 Recombinant proteins

N-terminally His_6- or His_7-tagged proteins EndoM N175Q (108), BgaA (109), SpHex (110), and FKP (111) were each expressed in *Escherichia coli* BL21(DE3) cells that were transformed with one of several plasmids (pET29-EndoM-N175Q, pET28-BgaA, p3AHEX-1.8, or pET15-FKP) which were provided by the lab of Stephen Withers (University of British Columbia), and cultured in LB medium. Cultures were grown to an OD_{600} of ~0.6 at 37 °C, at which point 0.5 mM isopropyl β-D-1-thiogalactopyranoside (IPTG) was added, following by overnight incubation at 18 °C. Cells were harvested by centrifugation and lysed by sonication. Each protein was purified from soluble cell extract using a 1 mL HisPur Ni-NTA column and the proteins were buffer exchanged into 20 mM sodium phosphate (pH 7.5) and 150 mM NaCl for storage (at 4 °C for up to two months or at -80 °C for longer).

Recombinant exo-α-neuraminidase from *Clostridium perfringens* (NanH) was purchased from New England Biolabs (P0720S), and chitinase from *Streptomyces griseus* was purchased from Millipore Sigma (C6137). Recombinant FUT8 was the kind gift of Kenta Yamato (Kaico Ltd.), Jae Man Lee (Kyushu University), and Takahiro Kusakabe (Kyushu University).

2.2Chromatography

2.2.1 Bio-Gel P-2 Gel

Bio-gel P-2 Gel was used as the resin in size exclusion columns (Bio-Rad, #1504118). The small size of the beads prevents particles over 45 μm from entering the beads. The estimated exclusion limit of the column is 100 to 1800 Da. The applied flow rate during size exclusion chromatography was 0.2 mL/min. 0.1 M ammonium bicarbonate was used as the elution buffer of sialoglycopeptide. Distilled water was used for the elution of oligosaccharides. UV signals were monitored at 234 nm and 280 nm since some of compounds absorbed UV light at those wavelengths. Loaded sample volumes were between 1 and 2 mL, allowing for sedimentation into the column before loading of buffer.

2.2.2 Carbon-celite column

A 1:1 slurry composed of 10 g Activated Charcoal (Fisher, #7440-44-0) and 10 g Celite (Fisher, #68855-54-9) was mixed in a beaker using a magnetic stir bar and used as the resin to pack the carbon-celite column. The applied flow rate was 0.2 mL/min with 25 % Acetonitrile (ACN) + 0.1 % TFA as the elution buffer. UV signals were monitored at 234 nm and 280 nm. Samples were loaded in volumes between 1 and 5 mL using a peristaltic pump and allowed to enter the resin completely before addition of buffers.

2.2.3 Sephadex G25

Sephadex G25 (Sigma-Aldrich, #G2580) was the resin used for size exclusion chromatography of sugar-oxazoline with beads size of 20 to 80 µm. The fractionation range is estimated at 1000 to 5000 Da. The flow rate was set at 0.2 mL/min and the elution buffer used was 0.01 % aqueous ammonia. UV signals were monitored at 234 nm and 280 nm. Samples loaded on the column had volumes of 1.5 mL and allowed to sediment into the column before addition of buffer.

2.2.4 Hydro-RP C-18

A reverse phase HyperSep C18 cartridge (ThermoFisher, 60108-301), containing particle sizes of 40 to 60 µm, was used for purifications of fluorogenic probe. Elutions were performed using solutions of 10 %, 20 % and 30 % methanol, with fractions collected by gravity; no flow rate was applied. Loaded sample volumes were 1 mL and allowed to sediment before applying buffers.

2.3 HPLC-MS analysis

2.3.1 Hydro-RP C18

Analysis was performed using an Agilent 1290 Infinity II UHPLC instrument in conjunction with an Agilent 6560 Ion Mobility Q-TOF mass spectrometer. Samples obtained from enzymatic assays were diluted 1:1 with distilled water, and 20 µl of each dilution was injected for chromatography using a Phenomenex 150 mm X 2.00 mm Synergi 4 µM Hydro-RP column. Samples were eluted from the column with the following gradient (buffer A being water + 0.1 % formic acid and buffer B being ACN + 0.1 % formic acid): 1 to 10 % buffer B at a flow rate of 0.3

mL/min over 4.0 min, 10 to 85 % buffer B at a flow rate of 0.3 mL/min over 1.0 min, 85 % buffer B at a flow rate of 0.4 mL/min for 1.2 min, 1 % buffer B at a flow rate of 0.4 mL/min for 2.1 min, and 1 % buffer B at a flow rate of 0.3 mL/min for 2.7 min. Detection of analytes by mass spectrometry was carried out by QTOF in negative mode with a source voltage of 2000 V and a scan rage of *m/z* 50 – 1750.

2.3.2 HILIC

Analysis was performed using an Agilent 1290 Infinity II UHPLC instrument in conjunction with an Agilent 6560 Ion Mobility Q-TOF mass spectrometer. Samples obtained from enzymatic assays were diluted 1:1 with ACN, and 20 µl of each dilution was injected for chromatography using a GlycanPac AXH-1 150 mm X 2.10 mm 3 µM HILIC column. Samples were eluted from the column with the following gradient (buffer A being 100 % ACN and buffer B being 100 % 80 mM Ammonium Formate pH 4.4): 1 to 10 % buffer B at a flow rate of 0.4 mL/min over 3.0 min, 10 to 20 % buffer B at a flow rate of 0.4 mL/min over 2.0 min, 20 to 55 % buffer B at a flow rate of 0.4 mL/min over 15.0 min, 55 % buffer B at a flow rate of 0.4 mL/min for 0.1 min, and 1 % buffer B at a flow rate of 0.4 mL/min for 6.9 min. Detection of analytes by mass spectrometry was carried out by QTOF in negative mode with a source voltage of 2000 V and a scan rage of *m/z* 50 – 1750.

2.3.3 Choice of column

Both Hydro-RP C18 and HILIC columns were tested for HPLC-MS analysis of enzymatic digestion reactions and demonstrated successful separation. The choice of column used was based on the availability of the column and showed no differences in capabilities for separation of analytes.

3 Results and discussion

3.1 Preparation of glycan and glycopeptide acceptor substrates for FUT8 from chicken egg yolk.

3.1.1 Background

A major obstacle in glycobiology research is the need for pure and easily accessible carbohydrates that can be studied. Despite the well-established importance of glycosylation, tools for studying glycans and general methods for the routine preparation of glycan substates are lacking (112). For this reason, various methods to produce these carbohydrate compounds have been developed (113). One such method involves the chemical or enzymatic deglycosylation of glycoproteins from natural sources, such as chicken egg yolk (114, 115). Chicken egg yolk is an abundant source of sialoglycopeptide (SGP), having an A2G2S2 structure attached to the pentasaccharide core of complex type *N*-glycans, where A stands for *N*-acetyl-glucosamine (GlcNAc), G stands for Galactose (Gal), and S stands for Neuraminic acid (Neu5Ac) (116) **(Figure 3.1)**. While natural sources are rich sources of glycans, the several purification steps involved make the procedures expensive, time consuming and produce only small yields of the desired product (117). In 2017, a recent study reported the isolation of gram quantities of homogenous SGP from commercially available egg yolk powder using solid/liquid extraction and hydrophilic-interaction-chromatography purification (118). The main advantages of this method are 1. the use

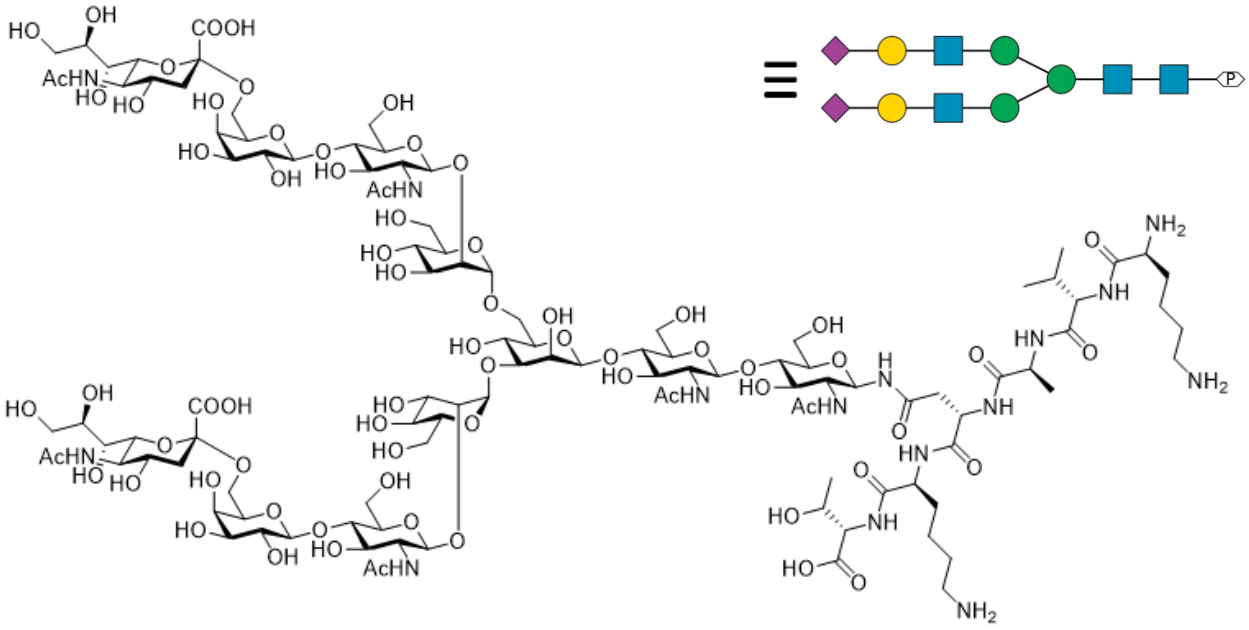

Figure 3.1. Chemical structure of Sialoglycopeptide.

of egg yolk powder instead of chicken eggs yolk which eliminates the need of cracking, separation and lyophilization of hundreds of eggs, and 2. the use of an active carbon/celite column which greatly reduces the amount of chromatography purification steps. We took advantage of this procedure to generate cheap and convenient starting materials to produce our FUT8 substrates.

3.1.2 Isolation of sialoglycopeptide

Our procedure for extracting SGP from egg yolk powder was adapted from the above report (118) and was further tweaked several times to arrive to an optimal procedure. Our initial attempt was carried out using 7 g of egg yolk powder, to validate the procedure described by Liu *et al.* (118). The ethanol washes and lipid extraction were performed using 13 mL of 95 % and 40 % ethanol respectively, and the crude SGP extract was chilled at 4 °C for 30 mins to precipitate proteins before being applied on an 8 mL carbon/celite column. The carbon/celite column was washed with 10 mL of 0 %, 5 %, and 10 % Acetonitrile (ACN) + 0.1 % TFA before eluting SGP with 10 mL of 25 % ACN + 0.1 % TFA. The fractions containing SGP were pooled, concentrated down to 1 mL by rotary evaporation, and purified on a 90 mL P-2 size exclusion column eluting with 0.1 M ammonium bicarbonate. This initial attempt resulted in a yield of 7 mg of SGP, or 1 mg per g of egg yolk powder. MS analysis of the product confirmed presence of SGP in the form of a doubly charged and triply charged species **(Figure 3.2)**.

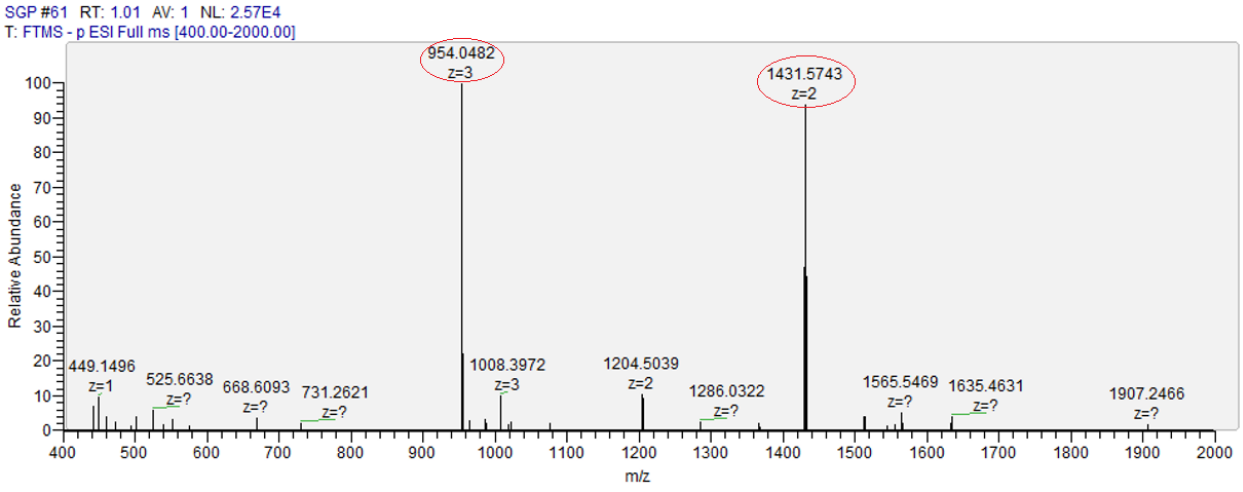

Figure 3.2. MS analysis of SGP extraction from chicken egg yolk. ESI-MS spectrum of the $[M - 2H]^{2-}$ ion at 1431.579 m/z and $[M - 3H]^{3-}$ ion at 954.050 m/z, both corresponding to SGP. Analysis was performed on purified of SGP.

Next, we were interested in scaling up the extraction protocol to allow us to generate hundreds of milligrams of SGP. For this reason, the first modification we made was the preparation of a 50 mL carbon/celite column that would be capable of separating a higher capacity of egg yolk powder. One issue that we encountered when applying a larger sample volume on the smaller 8 mL carbon/celite column was a diminished flow rate due to overpacking of the column, and we were able to resolve our column clogging issues by increasing the size of the carbon/celite column. To accommodate the increase in column volume, we also increased the volumes of our washes and elution steps (with ACN) to better separate SGP from the contaminants. Since the column volume was increased 6-fold from 8 mL to 50 mL, we increased the volumes of the washes and elution steps to 60 mL to keep approximately the same ratio.

Additionally, scaling up the starting SGP mass into the hundreds of milligrams would mean that the total filtrate collected could easily exceed 1 L volumes. This increase in volume necessitated changing the chilling conditions for protein precipitation. As such, we decided to change our protein precipitation step from 30 mins at 4 °C to an overnight chilling at -20 °C. Going from 4 °C to -20 °C allowed for the residual lipids remaining after extraction to coagulate together into a single mass that was easily removable using a spatula. Following centrifugation, the supernatant was resulted in a lime-yellowish color and clear of visible precipitates.

Lastly, the purification was performed using a gradient on an FPLC instrument, instead of a step gradient as previously described, to automate the overall procedure. The carbon/celite column, loaded with egg yolk extract, was first washed with 60 mL of distilled water + 0.1 % TFA, followed by an increasing gradient from 0 % ACN + 0.1 % TFA to 25 % ACN + 0.1 % TFA over 400 mL, and then SGP was eluted with 60 mL of 25 % ACN + 0.1 % TFA, all collected in fractions of 5.0 mL volume. Fractions were spotted on TLC and stained with *p*-anisaldehyde to identify presence of SGP and contaminants. Positive fractions were then developed on TLC using 2:1:1 BuOH/AcOH/H_2O, the SGP-containing fractions were pooled together, and the pool was concentrated down to a 5 mL volume by rotary evaporation. Finally, the concentrate was applied to a 90 mL P-2 size exclusion column, with the remainder of the procedure being the same as before. The exact same procedure as above was repeated for the second batch of SGP extract. Overall, this procedure resulted in 148 mg of SGP from 200 g of egg yolk powder (or 0.74 mg of SGP per g of egg yolk powder), with the closest yield obtained to the literature reported value of

0.8 mg SGP per g of egg yolk powder (118), and thus is the optimal procedure to use for future extraction.

3.1.3 Conversion of sialoglycopeptide into acceptor substrates for FUT8

As a preliminary test before the synthesis of our fluorogenic probe, we wanted to confirm the substrate recognition of FUT8. For this, we carried out the enzymatic digestion of our freshly generated SGP material and prepared two potential FUT8 substrates that were later used to test the enzymatic activity of FUT8 – the glycan-peptide (G0-hexapeptide) and the free glycan (G0). We used recombinant exo-α-neuraminidase from *Clostridium perfringens* (NanH) (119) to remove the sialic acid residues and recombinant exo-β-galactosidase from *Streptococcus pneumoniae* (BgaA) (109) to remove the galactose residues on the non-reducing end of SGP, yielding the G0-hexapeptide compound. In a parallel reaction, we repeated the enzymatic digestion using NanH and BgaA, but we also added peptide-*N*-glycosidase F (PNGaseF) (120) which cleaves the glycosidic bond between the peptide sequence and the oligosaccharide, producing the free glycan G0. Following enzymatic digestion, both G0 and G0-hexapeptide were purified on a 90 mL P-2 size exclusion column eluting with distilled water and resulted in yields of 2.7 mg and 3.6 mg respectively, from a starting mass of 8 mg of SGP. MS analysis of each product confirmed presence of the free glycan G0 **(Figure 3.3)** and of the glycopeptide G0-hexapeptide **(Figure 3.4)**.

3.1.4 Experimental details for preparing substrates for FUT8 from chicken egg yolk

3.1.4.1 SGP extraction and purification

Sialoglycopeptide (**SGP**) was extracted and purified from chicken egg yolk powder following previously reported procedures, with slight modifications (118). Prior to extraction, egg yolk powder was first washed with 95 % ethanol. A 200 g portion of egg yolk powder (Modernist Pantry) was suspended in 400 mL of 95 % ethanol and stirred at room temperature for 30 minutes. The mixture was filtered over a Buchner funnel and dried by suction using a water aspirator. The filtrate containing ethanol-soluble contaminants was discarded, whereas the dry material was resuspended in 400 mL of 95 % ethanol for an additional wash. The mixture was stirred for another 30 minutes and dried by suction, after which the filtrate was discarded, and the solid material saved for further extraction. To extract SGP, the solid material was suspended in 400 mL of 40 % ethanol

and stirred at room temperature for 30 minutes. The mixture was filtered and dried as before, and the filtrate containing SGP was collected. The solid material was subjected to a second extraction (with an additional 400 mL of 40 % ethanol) and the filtrates were pooled and chilled at -20 °C overnight (over 12 hours) to precipitate proteins, which were pelleted by centrifugation (10000

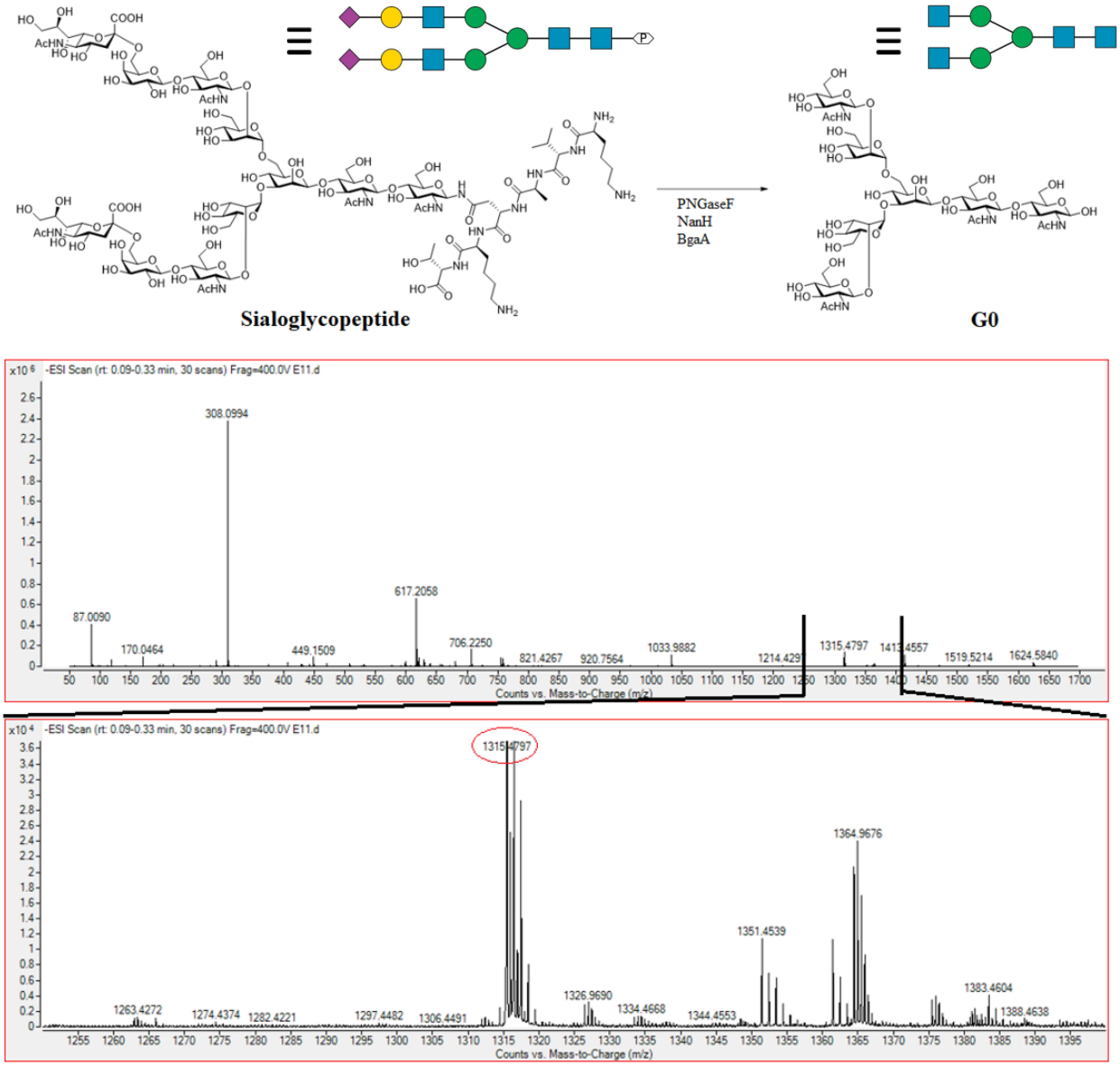

Figure 3.3. Preparation of G0 free glycan. Top: Scheme of enzymatic digestion of SGP to G0 using PNGaseF, NanH and BgaA. Bottom: ESI-MS spectrum of the $[M - H]^-$ ion at 1315.479 m/z, corresponding to G0. Analysis was performed following purification of enzymatic digestion reaction with PNGaseF, NanH and BgaA.

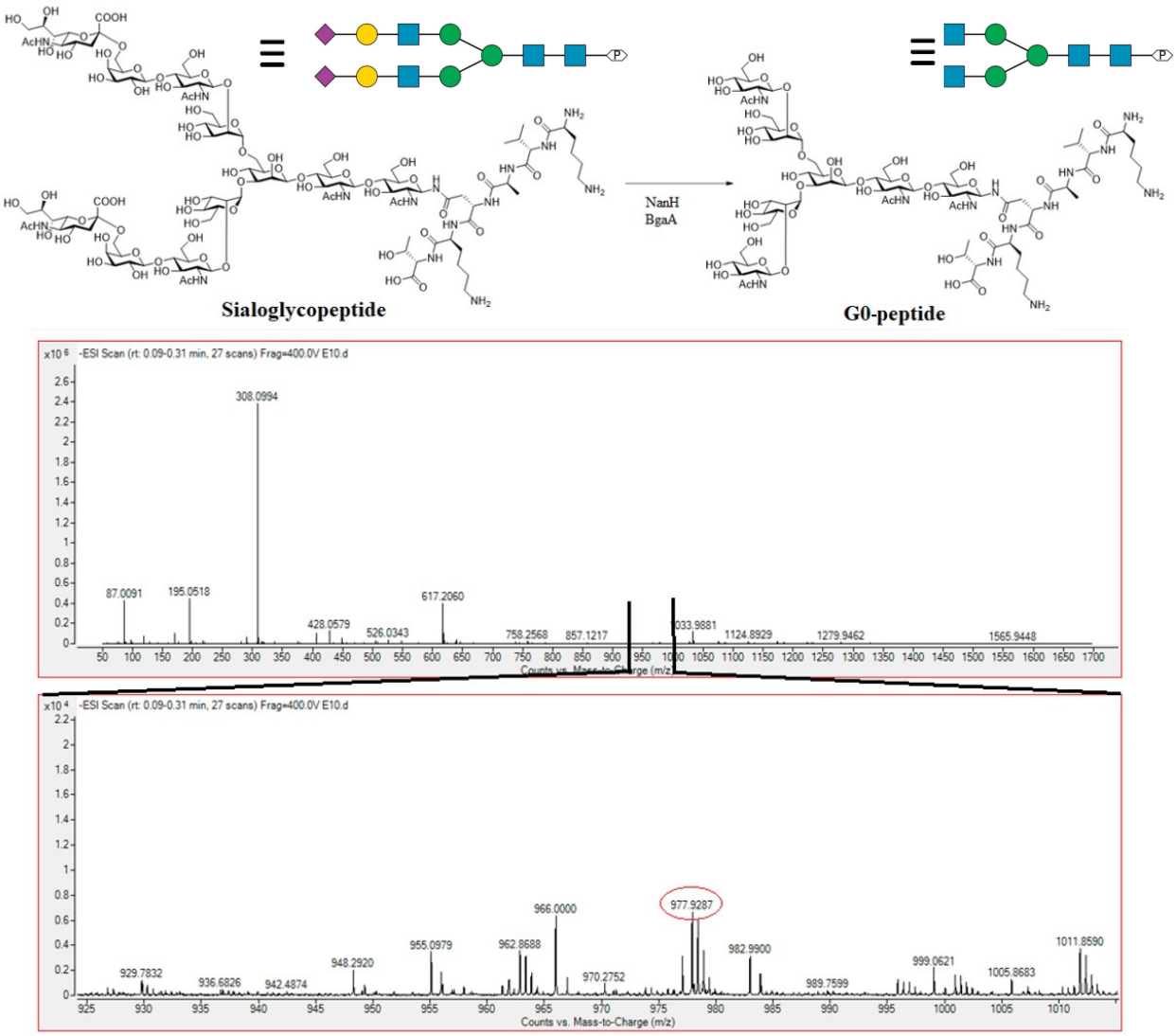

Figure 3.4. Preparation of G0-hexapeptide. Top: Scheme of enzymatic digestion of SGP to G0-hexapeptide using NanH and BgaA. Bottom: ESI-MS spectrum of the $[M - 2H]^{2-}$ ion at 977.930 m/z, corresponding to G0-hexapeptide. Analysis was performed following purification of the enzymatic digestion reaction with NanH and BgaA.

rpm, 4 °C, for 15 minutes). The supernatant was collected, separated in two and both batches were purified using the same procedure, as below. The supernatant was concentrated by rotary evaporation to 5 mL and applied to a 20 g (50 mL) carbon/celite column (1:1 by weight) that had been equilibrated with distilled water + 0.1 % TFA. The column was washed with 60 mL of distilled water + 0.1 % TFA, then eluted with a gradient between buffer A (distilled water + 0.1 % TFA) and buffer B (25 % ACN + 0.1 % TFA) as follows: 0 to 100 % buffer B over 400 mL followed by 100 % buffer B for 60 mL. The eluate was collected in 5.0 mL fractions, and those containing the desired material were identified by TLC and confirmed by mass spectrometry. SGP-

containing fractions were pooled and concentrated by rotary evaporation, then applied to a 90 mL P-2 size exclusion column previously equilibrated with 0.1 M ammonium bicarbonate. The column was eluted with 0.1 M ammonium bicarbonate, and fractions containing pure SGP were lyophilized to dryness, yielding a white, fluffy powder.

3.1.4.2 Preparation of G0

Preparation of G0 (free glycan) was performed in a one-pot reaction of 400 µL volume. Purified SGP (8.0 mg, 2.8 µmol) was dissolved into a 50 mM sodium phosphate-buffered solution containing 3000 U/mL of PNGaseF (New England Biolabs). To the same reaction were also added 300 U/mL of NanH (New England Biolabs) and 60 µg/ml of BgaA. The reaction was left to incubate at 37 °C overnight until complete digestion, cleaving off the sialic acids, galactose residues and the peptide portion of the glycoprotein. The reaction mixture containing the free glycan G0 was applied on a Bio-gel P-2 size exclusion column (90 mL resin) using distilled water as the eluent. Product-containing fractions were pooled and lyophilized to dry mass.

3.1.4.3 Preparation of G0-hexapeptide

A one-pot enzymatic preparation of G0-hexapeptide was carried out in a 400 µL reaction volume. Purified SGP (8.0 mg, 2.8 µmol) was dissolved into a 50 mM sodium phosphate-buffered solution. 300 U/mL of NanH (New England Biolabs) and 60 µg/ml of BgaA were added to the reaction and left to incubate at 37 °C overnight. Following complete digestion, cleaving off the sialic acids and galactose residues, G0-hexapeptide was purified on a Bio-gel P-2 size exclusion column (90 mL resin) with distilled water as the eluent. Fractions containing G0-hexapeptide were pooled and lyophilized to dry mass.

3.2 Synthesis of MU-G0 as a fluorogenic probe for FUT8 activity

3.2.1 Background

To develop a sensitive and specific enzymatic assay for FUT8 activity, we started from previously reported literature which described the use of synthetic fluorogenic oligosaccharides to probe for glycosidase activity in highly sensitive fluorescence-based assays (121, 122). In this work, Zhang *et al.* used a 4-methylumbelliferone fluorophore attached to the reducing end of oligosaccharides, which upon enzymatic hydrolysis catalyzed by specific glycosidase enzymes, would release the fluorophore and produce a detectable fluorescent signal. However, if the synthetic fluorogenic oligosaccharides were not treated with the specific glycosidases, the fluorophore would remain attached to the oligosaccharides and no fluorescence would be observed. This strategy could be adapted with slight adjustments to probe for the activity of glycosyltransferases (namely FUT8) instead of glycosidases. For this purpose, we sought to synthesize a fluorogenic oligosaccharide substrate that could be recognized by FUT8. Inspired from literature, we devised two strategies that could be used for the synthesis of our fluorogenic oligosaccharide **(Figure 3.5)**. The two strategies differ in the manner in which the oligosaccharide is coupled to the fluorogenic methylumbelliferyl moiety—one involves an $SnCl_4$-catalyzed chemical glycosylation to couple the oligosaccharide and fluorogenic tag (123) and the other involves chemo-enzymatic transglycosylation by a mutant endoglycosidase (124). Without knowing *a priori* which of these synthetic routes would be more successful or effective, we began with the first steps that the $SnCl_4$-catalyzed chemical glycosylation and the chemo-enzymatic transglycosylation share between them.

Since FUT8 recognizes the core *N*-glycan structure (Manα1–6(Manα1–3)Manβ1–4GlcNAcβ1–4GlcNAcβ), the first step in either strategy would be to generate an oligosaccharide structure that resembles a FUT8-substrate, starting from the naturally occurring sialoglycopeptide isolated from egg yolk powder. Both the $SnCl_4$-catalyzed chemical glycosylation and chemo-enzymatic transglycosylation routes require, as the first steps, enzymatic trimming of the sialoglycopeptide glycan to remove terminal sugar residues at the non-reducing branched ends followed by enzymatic cleavage at the reducing end of the oligosaccharide to remove the peptide portion of the molecule. In both cases, trimming of the sugars at the non-reducing branched ends makes use of a recombinant exo-α-neuraminidase from *Clostridium perfringens* (NanH) (119) to

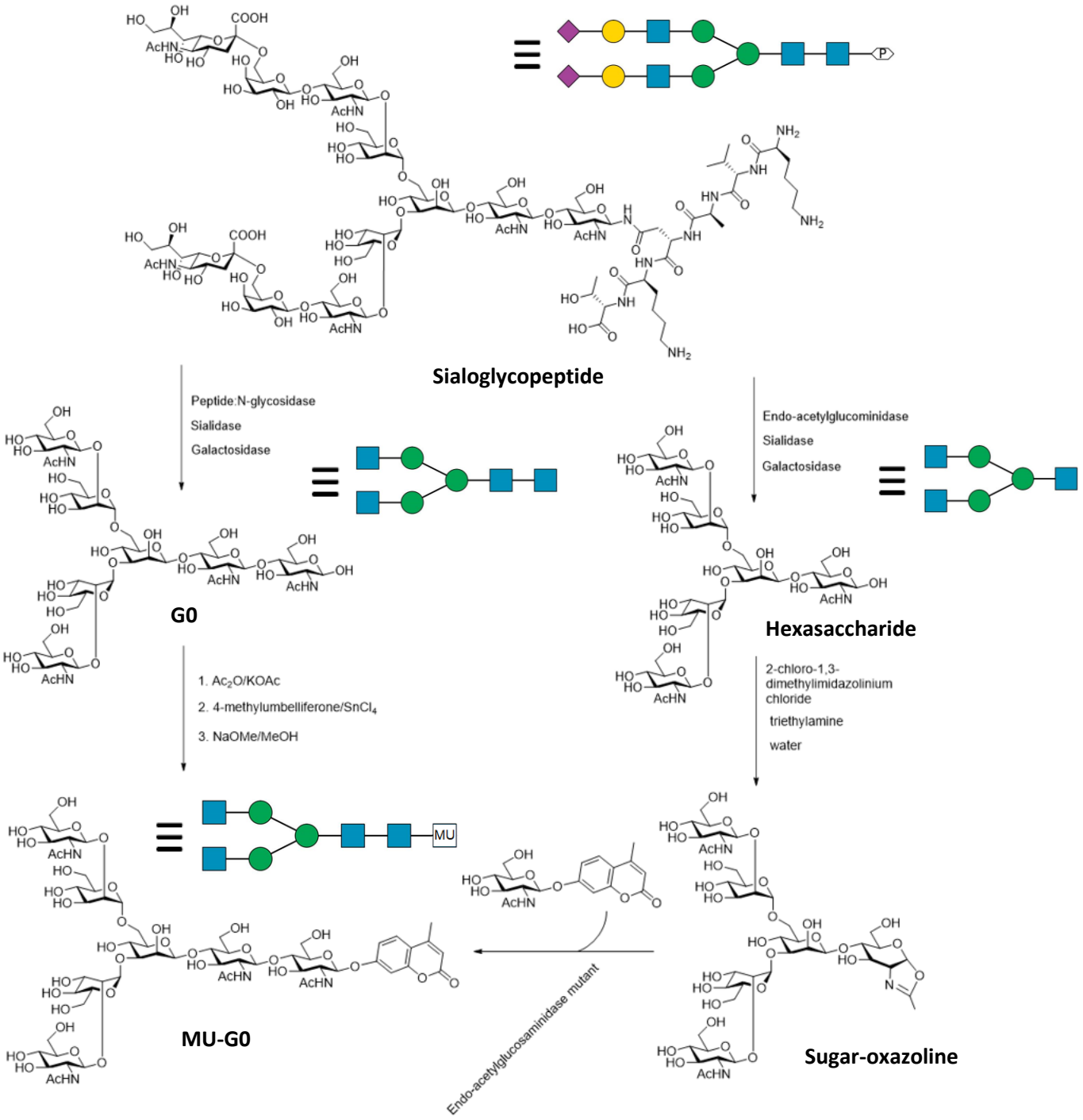

Figure 3.5. Proposed schemes for the synthesis of MU-G0 from SGP. Overview of the $SnCl_4$-catalyzed chemical glycosylation route (left branch) and chemo-enzymatic transglycosylation route (right branch).

remove the sialic acids residues, and a recombinant exo-β-galactosidase from *Streptococcus pneumoniae* (BgaA) (109) to remove the galactose residues. For the $SnCl_4$-catalyzed chemical glycosylation route, the oligosaccharide intermediate is generated by enzymatic hydrolysis at the reducing end, using a Peptide-*N*-glycosidase F (PNGaseF) (120), to cleave the peptide from the glycan and producing the heptasaccharide core structure (G0). Alternatively, for the chemo-enzymatic transglycosylation route an Endo-β-*N*-acetylglucosaminidase from *Mucor hiemalis* (EndoM) (124) is used to cleave the peptide with an *N*-acetylglycosamine residue producing a hexasaccharide structure, which is the core *N*-glycan structure with one less residue at the reducing end. Following purification of the produced glycan structures, coupling of either 4-methylumbelliferone to the reducing end of the heptasaccharide or 4-methylumbelliferyl β-*N*-acetylglucosamine to the reducing end of the hexasaccharide is performed to generate the synthetic fluorogenic oligosaccharide substrate **(Figure 3.5)**.

The two synthetic routes largely diverge in the coupling strategy by which a fluorogenic 4-methylumbelliferyl tag is installed on the oligosaccharide. In the $SnCl_4$-catalyzed chemical glycosylation route, the heptasaccharide product from the enzymatic digestions requires a protection step involving acetic anhydride before coupling can occur with the use of stannic (IV) tetra chloride. Following successful coupling, the generated glycoside would be deprotected using methanol in sodium methoxide and purified on column to yield the purified 4-MU-G0 probe. In the chemo-enzymatic transglycosylation route, the enzymatically trimmed hexasaccharide is used as a reagent in an oxazoline ring formation reaction with 2-chloro-1,3-dimethylimidazolinium chloride (DMC), producing an intermediate with an oxazoline functional group at the reducing end of the glycan. A transglycosylation reaction is then carried out on the sugar-oxazoline with a 4-methylumbelliferyl *N*-acetylglucosamine in the presence of an Endo-β-*N*-acetylglucosaminidase N175Q from *Mucor hiemalis* (EndoM-N175Q) mutant enzyme, which after purification yields the fluorogenic probe MU-G0.

3.2.2 $SnCl_4$-catalyzed chemical glycosylation route

While researching potential strategies for our probe synthesis, we came across a similar reaction reported by Huang G. L. (123) describing the synthesis of 4-methylumbelliferyl-penta-*N*-acetylchitopentaoside. The procedure involved a protecting group strategy, reacting a

chitooligosaccharide with acetic anhydride, to generate a peracetylated chitooligosaccharide. The collected peracetylated chitopentaoside was then reacted with 4-methylumbelliferone, using stannic (IV) tetra chloride as the catalyst, to generate the peracetylated methylumbelliferone chitopentaoside with the fluorophore group attached to the reducing end of the oligosaccharide. The fluorogenic product was deacetylated using sodium methoxide and purified on an ion-exchange column to yield the 4-methylumbelliferyl-penta-*N*-acetylchitopentaoside. Thus, the coupling reaction between 4-methylumbelliferyl and the oligosaccharide could be summarized in three major steps. The first, a protection step of all hydroxyl groups; the second, a coupling reaction at the reducing end using a Lewis acid catalyst; the last, a deprotection step to regenerate the hydroxyl groups. With this strategy in mind, we aimed to perform the coupling reaction between the heptasaccharide G0 and 4-methylumbelliferone.

Since we have already demonstrated production of the desired oligosaccharide G0 for the chemical coupling reaction, we decided to scale up our procedure to generate more of the oligosaccharide material. As such, 40.2 mg of purified SGP was dissolved in a 50 mM sodium phosphate-buffered solution containing 3000 U/mL of PNGaseF, 300 U/mL of NanH and 50 µg/ml of BgaA. The reaction was left to incubate at 37 °C overnight until complete digestion then purified on a Bio-gel P-2 size exclusion column (90 mL resin) using distilled water as the eluent. Product-containing fractions were pooled and lyophilized to dry mass to yield 27.9 mg of G0 **(Figure 3.6)**. Following production of our G0 compound, we looked to perform the $SnCl_4$-catalyzed chemical glycosylation as was described by Huang. G. L. (123) **(Figure 3.7)**. In the first protection reaction with acetic anhydride, the hydroxyl groups would be replaced by acetate groups. We would then react the peracetylated G0 with 4-methylumbelliferone using stannic (IV) tetra chloride. Lastly, the hydroxyl groups would be regenerated by adding sodium methoxide to the mixture and purifying our compound. However, once we had performed the enzymatic trimming to produce our G0 core *N*-glycan structure we found ourselves at a crossroads as to whether proceed with the chemical glycosylation strategy, or instead attempt the chemo-enzymatic transglycosylation.

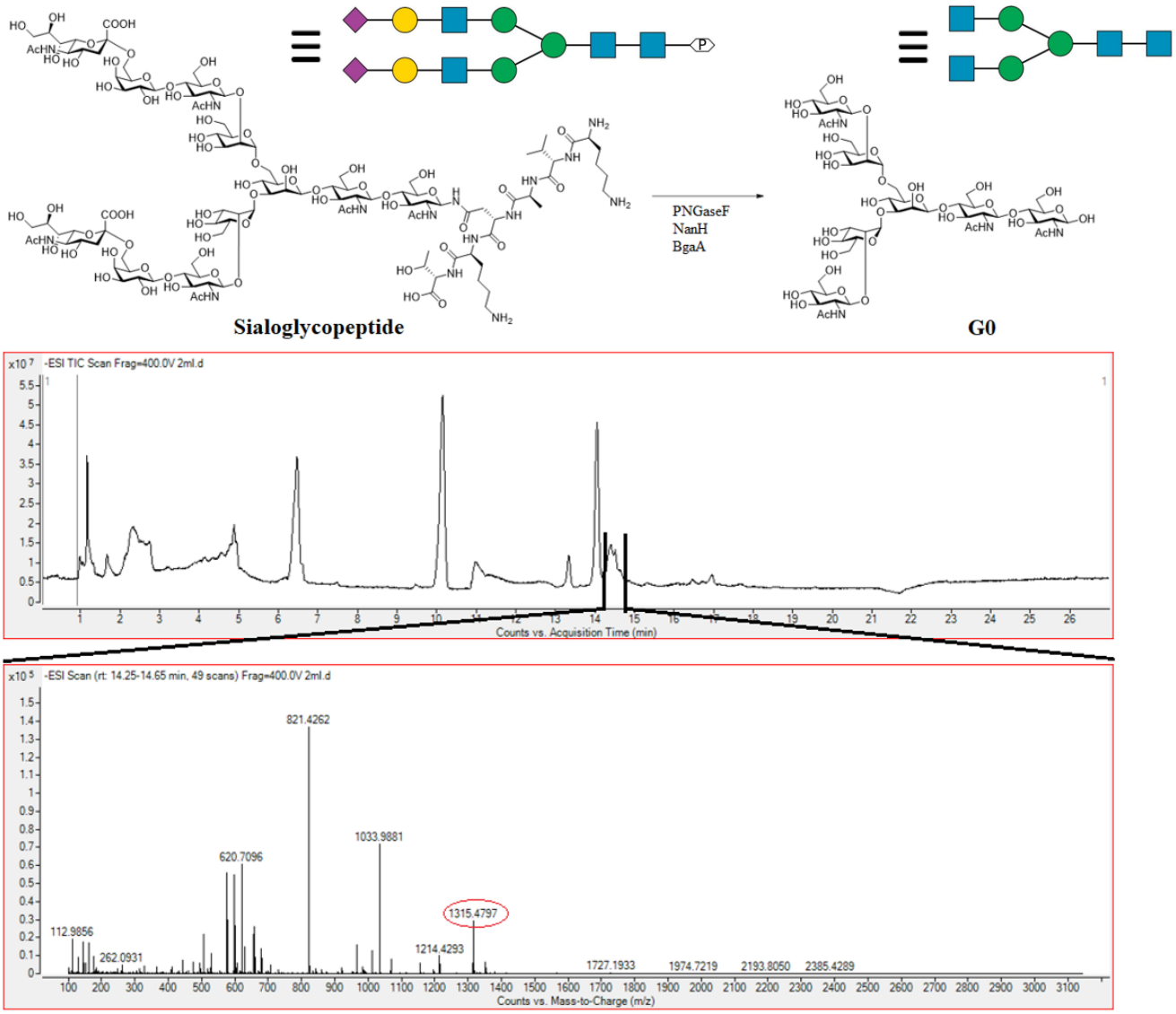

Figure 3.6. Enzymatic digestion reaction for the $SnCl_4$-catalyzed chemical glycosylation route. Top: Scheme of the enzymatic digestion reaction of *SGP* into *G0* using PNGaseF, NanH and BgaA. Bottom: LC-MS chromatogram of the peak containing G0 and LC-MS/MS spectrum of the $[M - H]^-$ ion at 1315.479 m/z, corresponding to G0. Analysis was performed following purification of enzymatic digestion reaction with PNGaseF, NanH and BgaA.

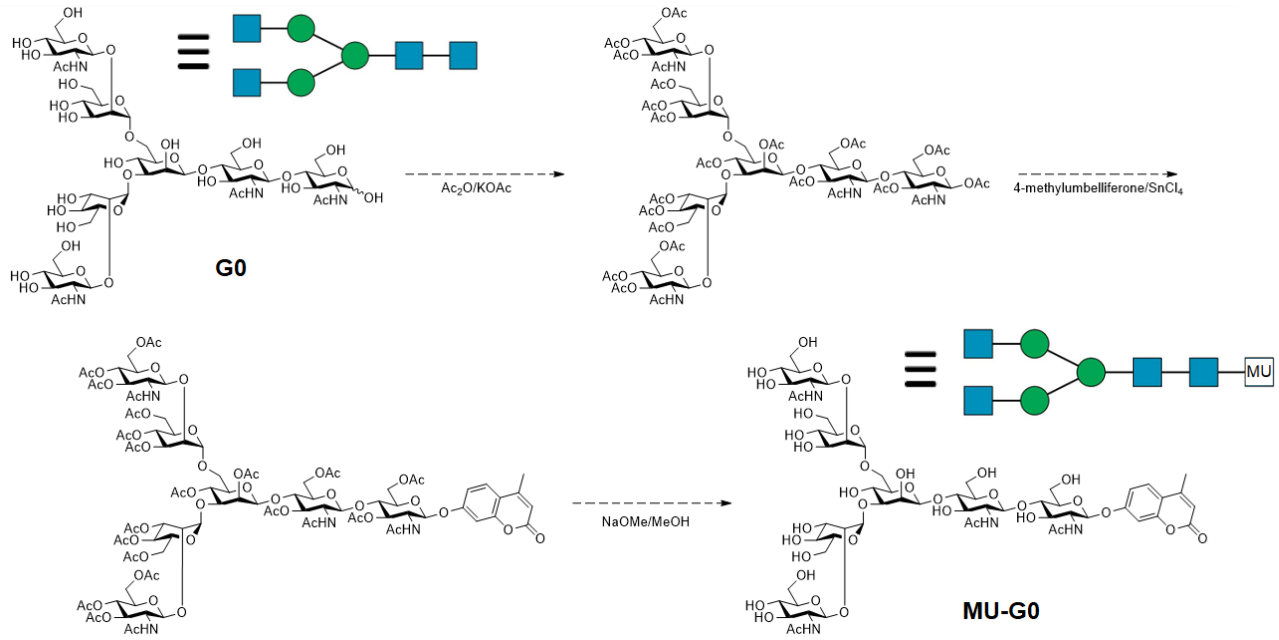

Figure 3.7. Scheme for the chemical glycosylation of 4-methylumbelliferone with G0 into MU-G0 in the $SnCl_4$-catalyzed chemical glycosylation route.

We weighed the alternatives and took several points into consideration. Firstly, when performing organic synthesis with a complex oligosaccharide such as G0, there is a risk of creating undesired side products; this is critical due to the number of hydroxyl groups that need to be protected then deprotected, making the reaction very tedious. Secondly, although the desired β-anomer is predicted to be favored in the $SnCl_4$-catalyzed chemical glycosylation, control over the regioselectivity of the glycosidic bond between the fluorophore and the oligosaccharide is not absolute, yet it is imperative for the bond to be in the β-orientation to be recognized by FUT8. It is very difficult to separate the two anomers from one another, and thus an enzymatic coupling with strict regioselectivity may be favorable compared to a chemical coupling. Lastly, the coupling reaction necessitates the use of stannic (IV) tetra chloride as the Lewis acid catalyst which is a very hazardous compound. In an age where a big emphasis is placed on green chemistry and environmentally friendly reactions, this step breaks several principles of green chemistry, thus making the coupling strategy less favorable. With these factors in mind, we decided to put this strategy on hold and attempt the chemo-enzymatic transglycosylation route first.

3.2.3 Chemo-enzymatic transglycosylation route

As with the $SnCl_4$-catalyzed chemical glycosylation route, the chemo-enzymatic transglycosylation strategy was based on previous literature. In a report by Umekawa *et al.* (124), the authors describe the utility of the transglycosylation activity of a mutant Endo-β-*N*-acetylglucosaminidase N175Q from *Mucor hiemalis* (EndoM N175Q) as a tool for glycoconjugate syntheses. This mutant enzyme is capable of performing efficient transglycosylation reactions on both sialo-complex sugar oxazolines and natural sialo-complex *N*-glycans (108). Since the sugar oxazoline is an intermediate formed during the two-step reaction mechanism of the transglycosylation catalyzed by EndoM, we hypothesized that using the sugar oxazoline as the starting material for our transglycosylation reaction would result in a higher yield. Thus, we turned to literature and found an article describing the synthesis of sugar oxazolines using 2-chloro-1,3-dimethylimidazolinium chloride (DMC) and triethylamine in water (125). Comparing to the chemical coupling strategy, the chemo-enzymatic reaction is carried out in water, allowing for a greener, less harmful, and abundant solvent; the reaction is also less harsh because it uses an enzyme as the catalyst instead of a reactive chemical catalyst. One concern with using DMC is the release of hydrochloric acid over the course of the reaction, but the triethylamine can neutralize the molecules of hydrochloric acid because it is added in excess. Thus, with the transglycosylation reaction and oxazoline synthesis in mind, the missing piece is generating the oligosaccharide reagent for the oxazoline reaction, which will be produced by enzymatic digestion of SGP as was demonstrated previously.

It is worth mentioning here that the glycan precursor in the chemo-enzymatic transglycosylation reaction is a hexasaccharide structure, which is the oligosaccharide G0 with one less acetylglucosamine residue at the reducing end. As such, 18.0 mg of purified SGP was dissolved in 50 mM of sodium phosphate-buffered solution containing 300 U/mL of NanH, 50 μg/ml of BgaA and 50 μg/ml of EndoM. The reaction was incubated at 37 °C overnight and purified on a Bio-gel P-2 size exclusion column, eluting with distilled water. From this reaction was recovered 5.7 mg of hexasaccharide **(Figure 3.8)**. This is a much lower yield compared to enzymatic digestion in the chemical coupling strategy. We reasoned that this difference may be due to the usage of EndoM, instead of PNGaseF, which has an optimal temperature of 30 °C despite

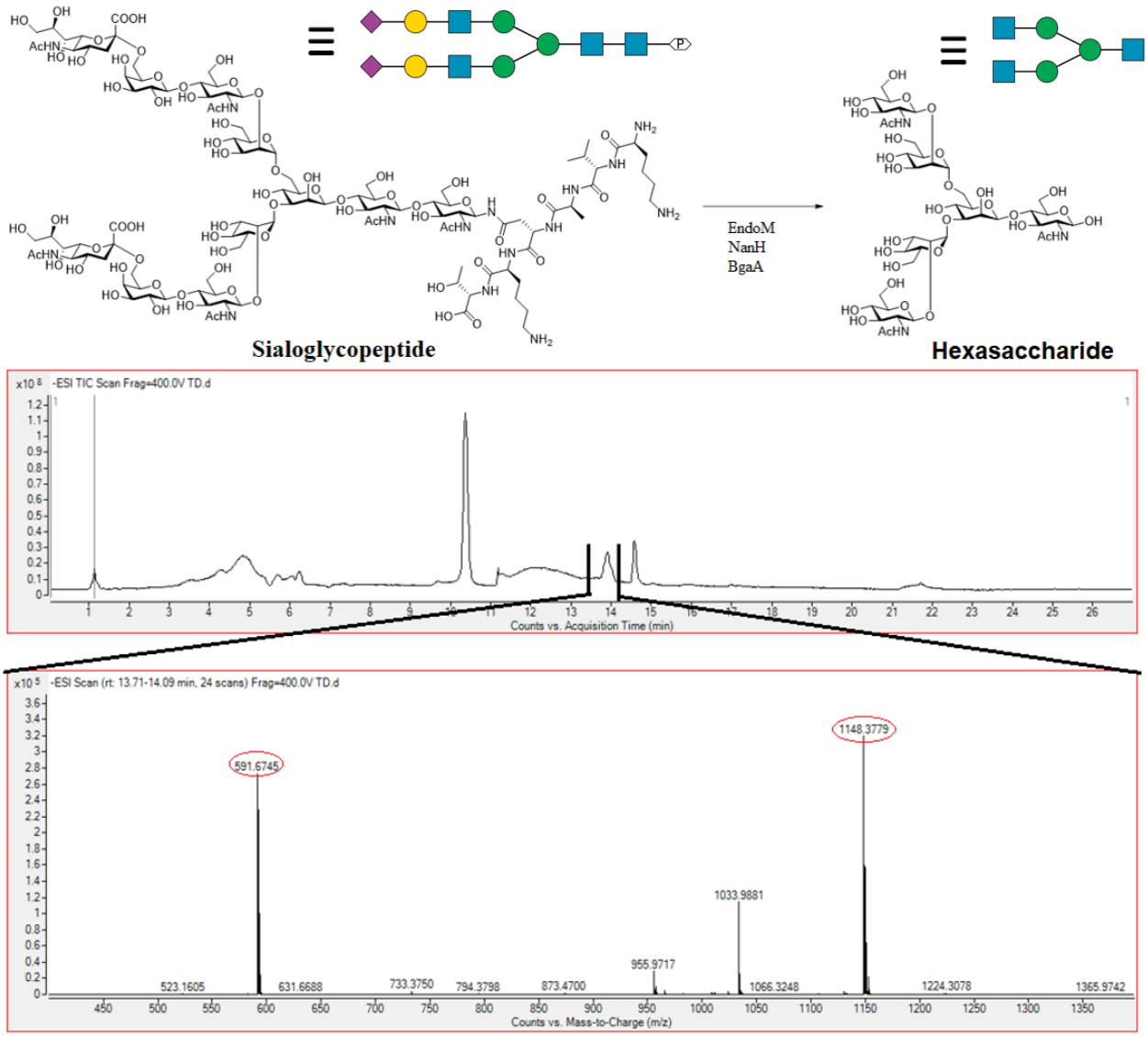

Figure 3.8. Enzymatic digestion reaction for the chemo-enzymatic transglycosylation route. Top: Scheme for the enzymatic digestion reaction of SGP into Hexasaccharide using EndoM, NanH and BgaA. Bottom: LC-MS chromatogram of the peak containing Hexasaccharide and LC-MS/MS spectrum of the $[M + Cl]^-$ ion at 1148.377 m/z and $[M – H + Cl]^{2-}$ ion at 591.673 m/z, corresponding to Hexasaccharide. Analysis was performed following purification of enzymatic digestion reaction with EndoM, NanH and BgaA.

being reported as functional at 37 °C (108). Therefore, for future reactions, we decided to perform the enzymatic digestions at the reducing end first, using EndoM, and at the non-reducing end last, using NanH and BgaA.

The next step in the chemo-enzymatic synthesis was to generate the oxazoline ring at the reducing end of our hexasaccharide to be used as the substrate for the transglycosylation reaction to follow. We repeated the above enzymatic digestion reactions a few more times in order to obtain

sufficient starting material to produce at least one milligram of the fluorogenic probe product. We pooled all of our purified hexasaccharide products before proceeding. Thus, 14.1 mg of hexasaccharide was dissolved in 1 mL of distilled water and chilled on ice. To the solution was added 220 µL of triethylamine and 90.1 mg of DMC, and the mixture was stirred using a magnetic stir bar for 1 hour on wet ice. In this reaction, triethylamine works by abstracting a proton from the hemiacetal hydroxyl group at the reducing end, thus allowing the oxygen anion to react with DMC and form a reactive intermediate. This then leads to the carbonyl oxygen of the 2-acetamido group to perform an intramolecular attack on anomeric carbon and form the oxazoline ring. The reaction between the hemiacetal oxygen and DMC can occur in both in the α and β configuration (125), however intramolecular ring formation is sterically prohibited in the α configuration (125) and the reactive intermediate is hydrolyzed to regenerate the free sugar and DMC. Thus, this reaction effectively allows to solve the regioselectivity issue that occurred in the chemical coupling strategy. Once the ring formation reaction was completed, the mixture was purified on a Sephadex G10 column using 0.01 % ammonium hydroxide as the eluent and immediately freeze dried to dry mass, since the sugar-oxazoline product is rather unstable in solution, for a yield of 5.5 mg of product **(Figure 3.9)**.

The final step of the coupling strategy is the transglycosylation reaction of MU-GlcNAc with the hexasaccharide-oxazoline to generate the synthetic fluorogenic oligosaccharide MU-G0. The key component in this reaction is the mutant enzyme EndoM N175Q. While the wild type EndoM has a higher hydrolytic activity, the mutant enzyme has an abolished hydrolytic activity due to the amino acid mutation, and consequently has a much higher transglycosylation activity, which was only minimally observed in the wildtype enzyme (108). Furthermore, since MU-GlcNAc is a cheap and commercially available reagent, we supplied this reagent in excess, to ensure that our hexasaccharide-oxazoline was the only limiting reagent in our transglycosylation reaction. Thus, 0.7 mg of hexasaccharide-oxazoline was dissolved in a 50 mM sodium phosphate-buffered solution containing 300 µg/mL of EndoM N175Q. To the solution was added 10 mM MU-GlcNAc in 100 % DMSO (for a final DMSO concentration of 10 %) and the reaction was incubated at 30 °C for 20 mins. Afterwards, 50 µg/mL of exo-β-*N*-acetylhexosaminidase from

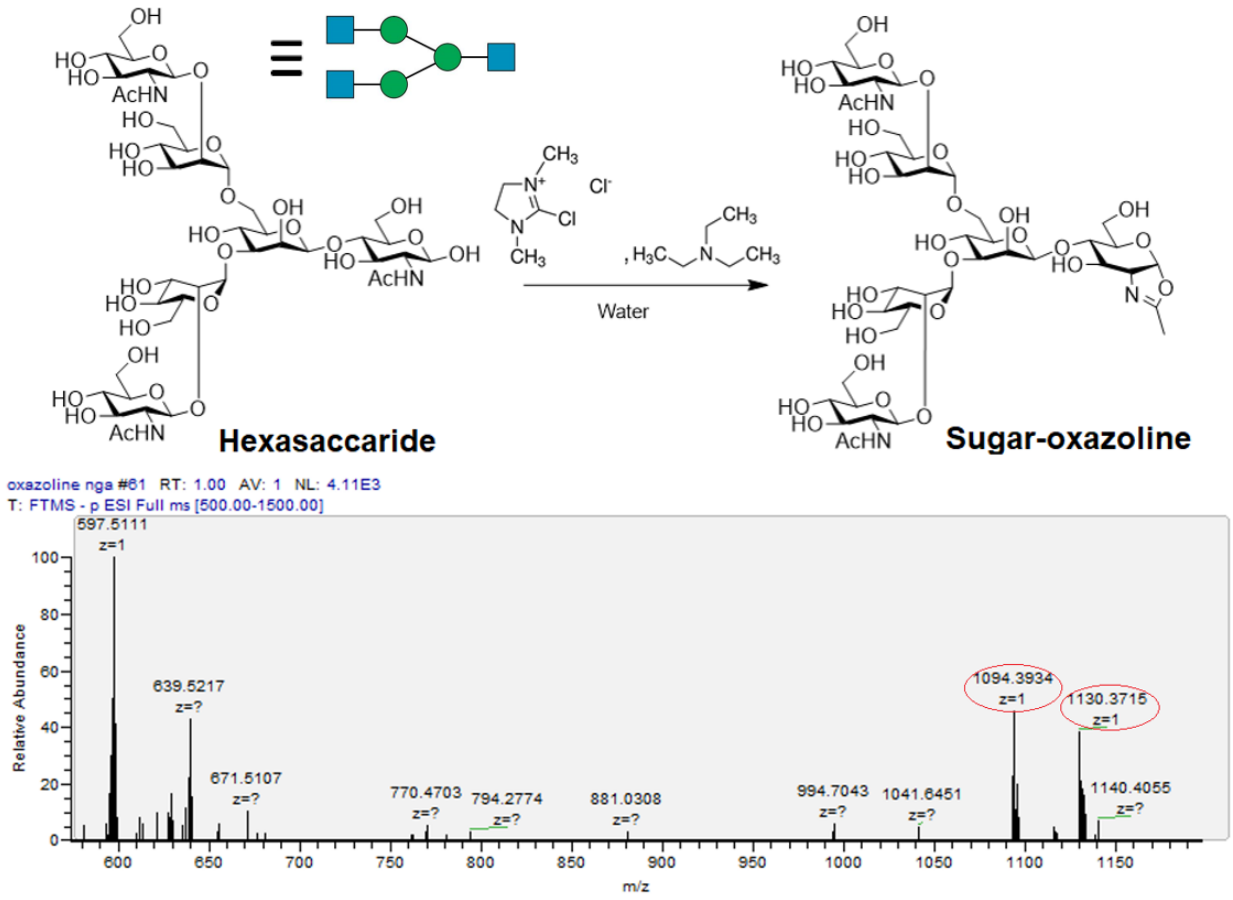

Figure 3.9. Oxazoline synthesis reaction in the chemo-enzymatic transglycosylation route. Top: Scheme for the synthesis of sugar-oxazoline from Hexasaccharide. Bottom: ESI-MS spectrum of the $[M - H]^-$ ion at 1094.389 m/z and $[M + Cl]^-$ ion at 1130.365 m/z, corresponding to sugar-oxazoline. Analysis was performed following purification of product from the oxazoline synthesis reaction.

Streptomyces plicatus (SpHex) was added to digest any unreacted MU-GlcNAc (into the free acetylglucosamine sugar and the free 4-methylumbelliferone) and the solution was reacted at 37 °C for 30 mins. Once the reaction completed, the enzymes were heat-inactivated at 95 °C for 5 mins and the whole mixture was loaded onto a C18 reverse phase column, washed with 10 mL of 0 % and 10 % methanol, and eluted with 20 % methanol. Fractions containing the MU-G0 product were pooled and lyophilized to dry mass, as well as analyzed by mass spectrometry **(Figure 3.10)**. This reaction yielded only 4.5 µg of MU-G0, as determined by a MU fluorescence standard curve. Unfortunately, we had several unsuccessful attempts before finally achieving the transglycosylation reaction, thus we were unable to repeat the chemo-enzymatic transglycosylation strategy with more starting material. Due to the complexity and challenges we encountered previously, we decided to modify our strategy altogether.

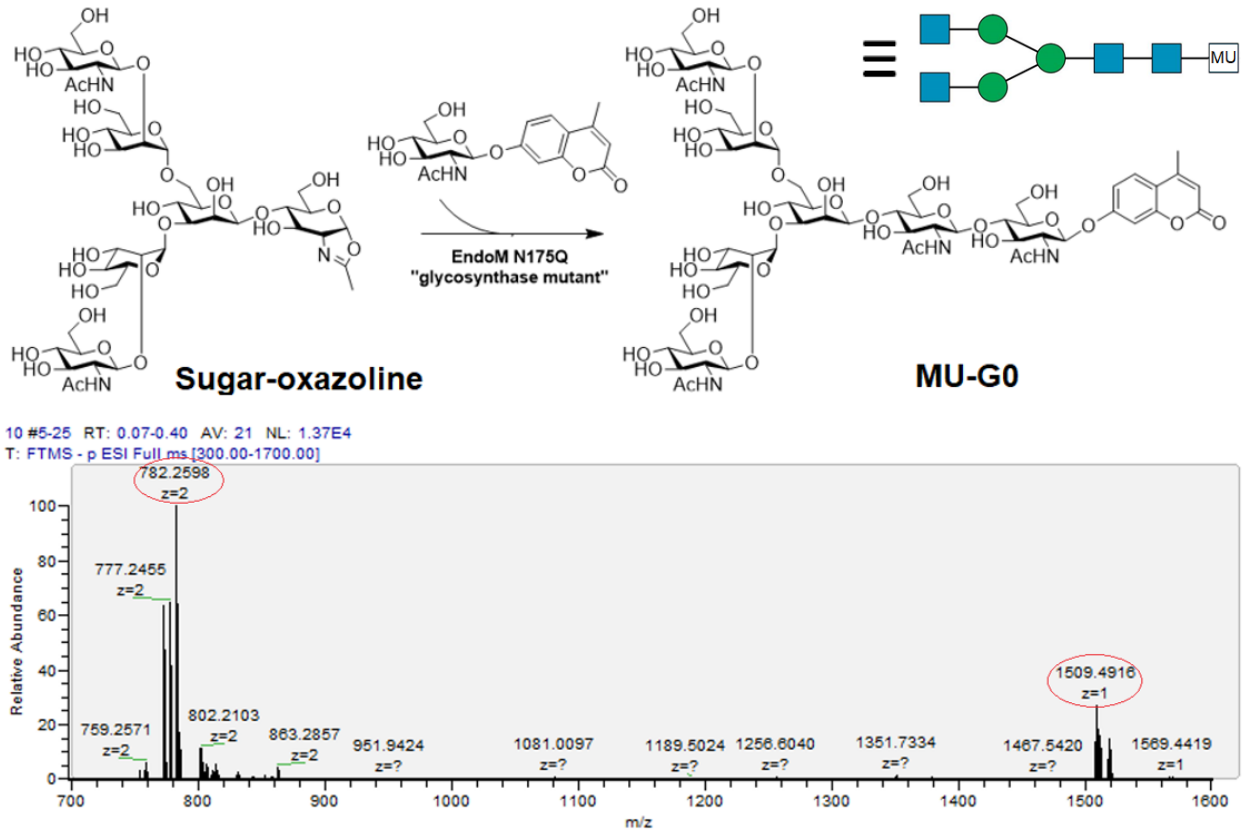

Figure 3.10. Transglycosylation reaction in the Chemo-enzymatic transglycosylation route. Top: Scheme for the transglycosylation reaction of sugar-oxazoline into MU-G0 using EndoM N175Q. Bottom: ESI-MS spectrum of the $[M + Cl]^-$ ion at 1509.492 m/z and $[M + 2\ formate]^{2-}$ ion at 782.256 m/z, corresponding to MU-G0. Analysis was performed following purification of product after performing the transglycosylation reaction.

3.2.3.1 Improved Chemo-enzymatic transglycosylation route on natural N-glycan

One issue with the chemo-enzymatic transglycosylation strategy is the several column chromatography purification steps in the procedure which are in great part responsible for lowering the final yield of the fluorogenic product. Unfortunately, it is not possible to cut out any of the purification steps in the procedure. The first purification step after enzymatic digestion of SGP is crucial for separating the hexasaccharide compound of interest from any asymmetrically cleaved oligosaccharides and free glycans that may act as substrates for the subsequent oxazoline ring formation reaction. The second purification step is necessary to remove the DMC-byproduct salt as the salt directly inhibits the transglycosylation reaction catalyzed by EndoM N175Q (124). The third purification yields the final product, and it is imperative to remove any unreacted reagents

from the final product in order to have an exact yield. Thus, while this chemo-enzymatic strategy was successful in generating the fluorogenic probe, it is far from optimal.

Fortunately, by making a few small changes to our chemo-enzymatic coupling strategy, we were able to improve our strategy procedure as well as resolving several of the initial issues. As was reported by Umekawa *et al.* (108), the EndoM N175Q mutant is capable of transferring oligosaccharides from both the sugar oxazoline and the natural sialoglycopeptide glycan. We reasoned that working with the sugar oxazoline would result in a potentially higher yield since it is an intermediate of EndoM N175Q, but since our result did not fit this hypothesis, we decided to work with the natural glycan instead. As such, 5.3 mg of MU-βGlcNAc and 8.0 mg of purified SGP were added into a sodium phosphate-buffered solution containing 0.5 mg/mL of EndoM N175Q and 10% DMSO, and the mixture was incubated overnight at 30 °C to generate MU-G2S2. When the reaction appeared to have reached completion, SpHex was added to the solution and the reaction was further incubated at 37 °C for an hour prior to heat-inactivation at 75 °C for 10 minutes. Afterwards, exo-α-neuraminidase (NanH) and exo-β-galactosidase (BgaA) were added to the reaction and left to incubate at 37 °C overnight to generate the product of interest, MU-G0. After complete digestion, MU-G0 was purified by a combination of liquid-liquid extraction using a 1:1 volume of ethyl acetate and reverse phase chromatography carried out with a stepwise gradient of increasing aqueous methanol. Finally, pooled fractions of MU-G0 were lyophilized to dry mass, yielding 2.5 mg of MU-G0 **(Figure 3.11)**.

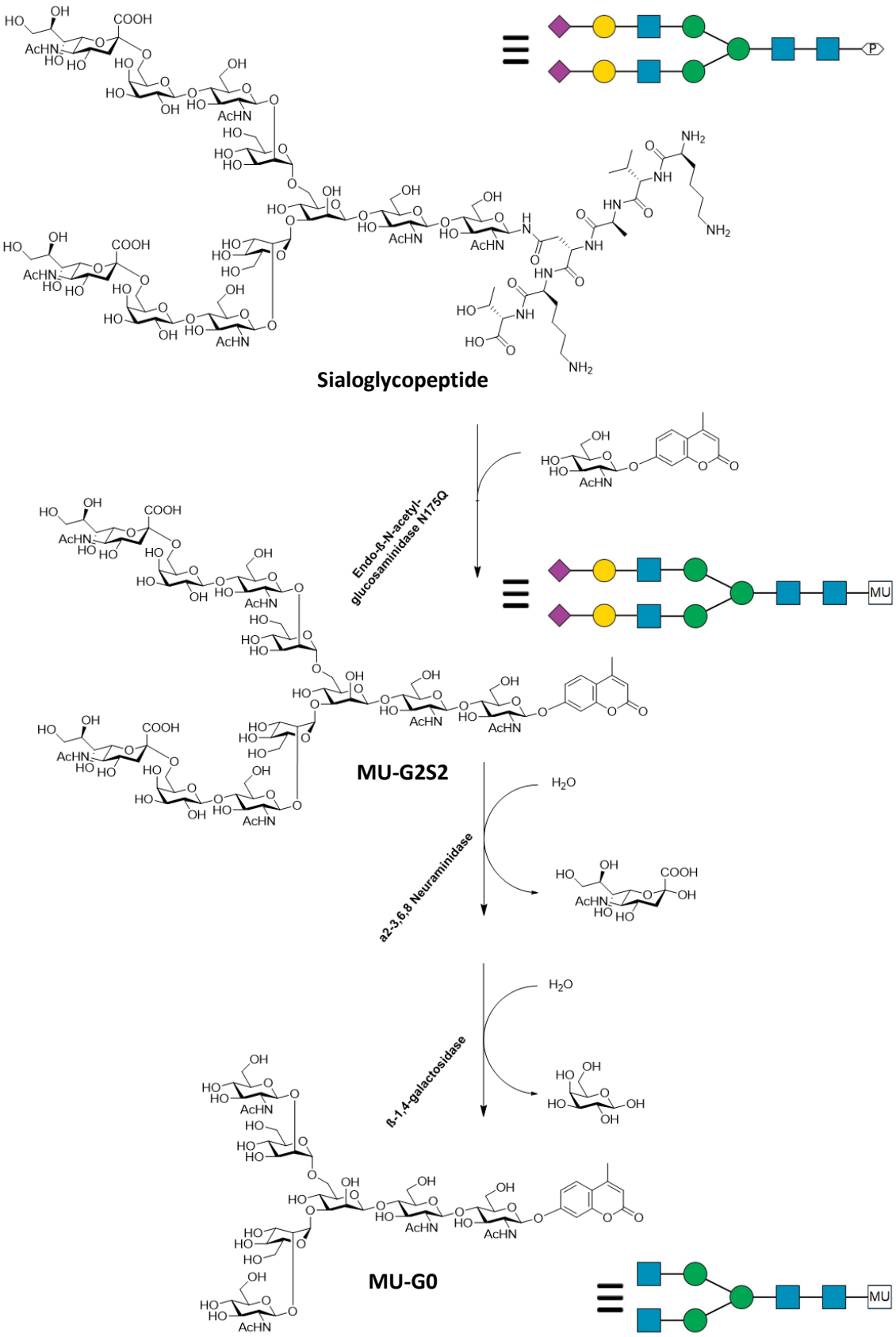
Sialoglycopeptide
Endo-ß-N-acetyl-glucosaminidase N175Q
MU-G2S2
a2-3,6,8 Neuraminidase
ß-1,4-galactosidase
MU-G0
MU
P

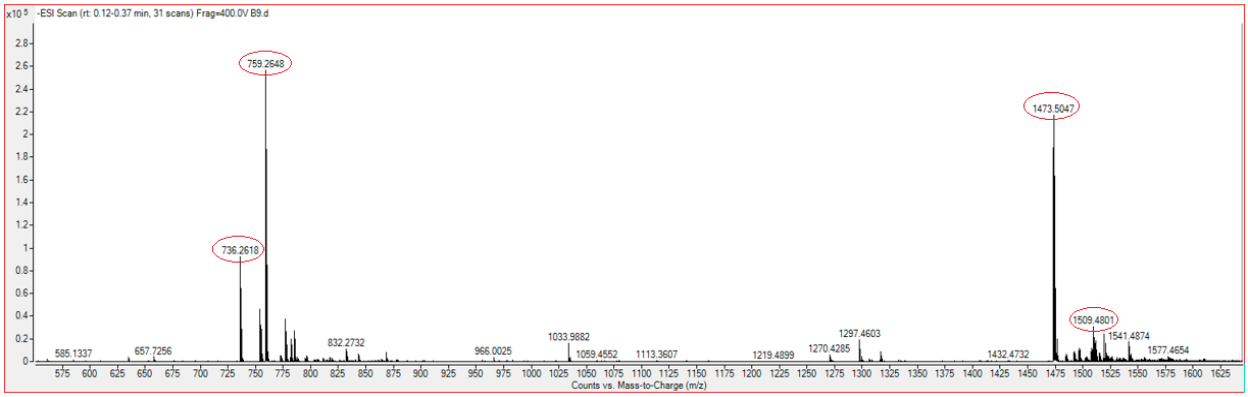

Figure 3.11. Improved chemo-enzymatic transglycosylation route. Top: Scheme for the improved chemo-enzymatic transglycosylation route of MU-G0 starting from SGP and MU-βGlcNAc using wild-type and engineered glycosidases. Bottom: ESI-MS spectrum of the $[M - H]^-$ ion at 1473.516 m/z, $[M + Cl]^-$ ion at 1509.492 m/z, $[M – 2H]^{2-}$ ion at 736.254 m/z, and $[M – H + formate]^{2-}$ ion at 759.257 m/z, all corresponding to MU-G0. Analysis was performed following purification of product after performing the translgycosylation and enzymatic digestion reactions.

There are a few advantages of using this method over the other two previously described. Compared to the $SnCl_4$-catalyzed chemical glycosylation route, this method does not have any organic synthesis reactions to generate any intermediates as the EndoM N175Q mutant acts directly on the natural sialoglycopeptide, thus the overall procedure is much greener. Additionally, there is no risk of side product formation as the transglycosylation reaction can only generate the MU-G2S2 product; and any unreacted MU-G2S2 or asymmetrically digested MU-G0 side products from the enzymatic digestions can be recovered and reprocessed again in subsequent trimming reactions. Lastly, since the reaction is enzyme-catalyzed, there is no need to worry about regioselectivity control because the MU-GlcNAc starting material can be purchased in its β-orientation. Compared to the initial chemo-enzymatic coupling strategy, this method begins directly with the transglycosylation reaction and follows up with the enzymatic digestion reactions, allowing to effectively cut down the number of chromatography purification steps from three to only one, which were the main culprits in reducing the final product yield. Furthermore, the added liquid-liquid extraction step facilitates the purification of MU-G0 from the free 4-methylumbelliferone since the fluorophore will be found in the organic phase and the probe will be in the aqueous phase. Several liquid-liquid extractions will be necessary to fully remove 4-methylumbelliferone from the solution since the compound is in excess in the reaction, but fortunately this is a quick and easy extraction step and is much less time consuming than another column chromatography. Finally, while we demonstrated the possibility of generating our

fluorogenic probe with the initial chemo-enzymatic transglycosylation strategy, the yield we recovered in our improved strategy was much greater than in the initial strategy, making it the much more favorable procedure to use.

3.2.3.2 Experimental Detail for synthesizing the MU-G0 probe

A multi-step one-pot synthesis of MU-G0 was carried out in a 500 µL reaction volume. First, 5.3 mg (51.5 µmol) of MU-βGlcNAc was dissolved in 200 µL of DMSO, and then added together with 8.0 mg (10.3 µmol) of purified SGP into a sodium phosphate-buffered solution containing 0.5 mg/mL of EndoM N175Q (with a final composition of 25 mM MU-βGlcNAc, 5 mM SGP, 0.5 mg/mL EndoM N175Q, 50 mM sodium phosphate buffered to pH 7, and 10 % DMSO), and the mixture was incubated overnight at 30 °C to generate MU-G2S2. Once no further formation of the MU-G2S2 intermediate was observed, SpHex was added to 0.07 mg/mL and the mixture was further incubated at 37 °C for an hour prior to heat-inactivation at 75 °C for 10 minutes. Addition of NanH to 0.4 µg/mL (40 U/mL), and BgaA to 0.15 mg/ml was followed by incubation at 37 °C overnight. After complete digestion, cleaving sialic acid and galactose residues, MU-G0 was purified by a combination of liquid-liquid extraction using a 1:1 volume of ethyl acetate to remove 4-methylumbelliferone, and chromatography using a reverse phase HyperSep C18 cartridge (ThermoFisher, 60108-301) carried out with a stepwise gradient of increasing aqueous methanol (6 mL steps of 0 %, 10 %, 20 %, 30 % methanol). Pooled, purified fractions of MU-G0 were lyophilized to dry mass.

3.3 Detection of FUT8-catalyzed fucosylation and development of a high-throughput fluorogenic assay of enzyme activity

3.3.1 Background

In previous work done by our research group (107), we developed a highly sensitive fluorescence-based assay for detecting the activity and inhibition of human fucosyltransferase VI (FUT 6). This assay, which was also adapted and modified from the glycosidase activity assay (121, 122), works by incubating fucosyltransferase and glycosidase reactions sequentially. When the 4-methylumbelliferyl oligosaccharide is first incubated with the fucosyltransferase, the resulting fucosylated product is no longer recognized by the glycosidases and no fluorescence signal is detected. However, if the fucosyltransferase is inhibited, fucosylation of the 4-methylumbelliferyl oligosaccharide is prevented, and the glycosidases can hydrolyze the oligosaccharide substrate, resulting in fluorescence detection of the released 4-methylumbelliferone.

Our research group sought to develop a similar assay for detecting the activity and inhibition of human fucosyltransferase VIII **(Figure 3.12)**, which is unique because it is the only enzyme capable of catalyzing core fucosylation, and as such has a completely different substrate than the other fucosytransferase enzymes. The aim of developing these assays is to address the lack of simple, robust and broadly applicable methods for performing high-throughput screening assays for glycosyltransferases. Some assays for detecting glycosyltransferase activity already exist, such as the detection of released nucleoside diphosphate or monophosphate from a glycosyltransferase reaction (126) or using fluorescently labeled nucleotide sugars to label glycans during transfer of the modified sugar nucleotides (127). The drawback with these assays is the need for the glycosyltransferase to recognize the modified donor substrate, or that the signal detected is not directly linked to the transfer of a sugar residue to the acceptor glycan substrate. Our system resolves these issues because the detectable signal is dependent on glycosylation of the acceptor glycan substrate and does not require modified donor substrates. Lastly, we performed an HPLC-based fucosyltransferase assay of FUT8 activity using G0 and G0-hexapeptide as the substrates to compare and validate the efficiency of our fluorescent based assay for measuring FUT8 activity. We have recently published this work (128).

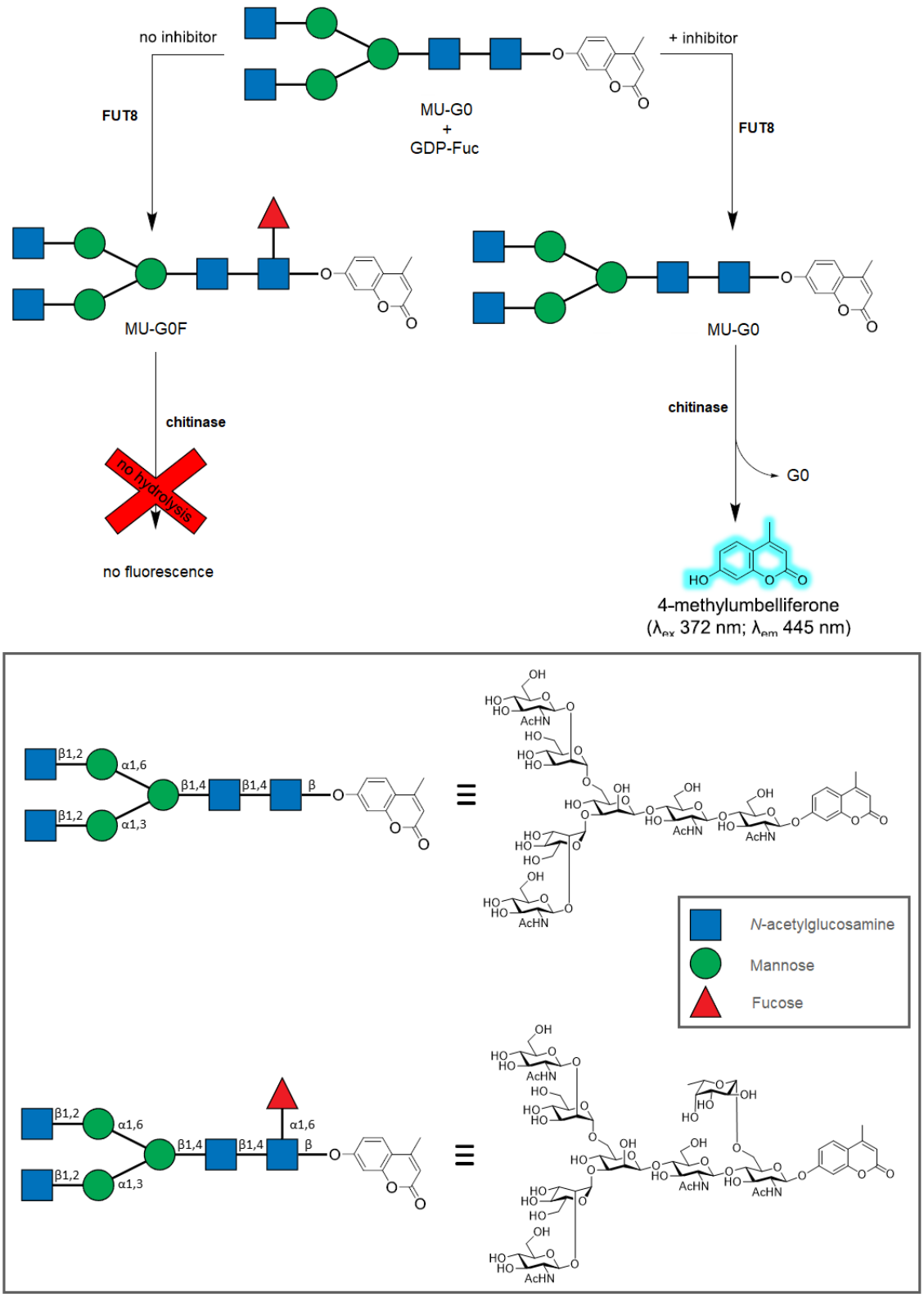

Figure 3.12. Fluorescence-based assay for testing FUT8 activity or inhibition. Inhibition is measured by the sequential incubation of FUT8 with MU-G0 and GDP-fucose in the presence or absence of an inhibitor, followed by chitinase for the specific hydrolysis of MU-G0.

3.3.2 HPLC-MS detection of fucosylation with glycan and glycan-peptide acceptor substrates

To test the activity of the recombinant FUT8 enzyme, we carried out fucosyltransferase assays using oligosaccharide G0 and glycopeptide G0-hexapeptide substrates, that we obtained from the enzymatic hydrolysis of sialoglycopeptide extracted from egg yolk powder. FUT8-catalyzed fucosylation of these substrates will add a fucose residue to the 6-OH of the *N*-acetylglucosamine (GlcNAc) residue at the reducing end, yielding the fucosylated products G0F or G0F-hexapeptide from the fucosylation of G0 or G0-hexapeptide, respectively.

We performed our reactions at 37 °C with 0.5 mM of acceptor substrates G0-hexapeptide or G0 (free glycan) and 1 mM of GDP-fucose donor substrate in a 50 mM sodium phosphate-buffered solution containing 20 μg/mL of FUT8 over two hours, collecting aliquots at different time points and heat inactivating at 95 °C to stop the reactions. HPLC–MS analysis **(Figure 3.13)** shows our results of the FUT8-catalyzed fucosylation of both G0 and G0-hexapeptide over time. As the reaction progresses, G0 is catalyzed by FUT8 and converted into fucosylated G0 (G0F). This is observed by the decrease of the relative abundance of G0 and the increase of the relative abundance of G0F. Similarly, G0-hexapeptide is converted into the fucosylated G0-hexapeptide (G0F-hexapeptide) and the same reaction effect can be observed.

In previous studies, the kinetics of recombinant FUT8 purified from *Sf21* cells (104) and native human FUT8 purified from MKN45 cells (99) were determined to be (12.9 ± 1.2) μM for the K_M of the oligosaccharide acceptor substrate and (19.3 ± 3.1) μM for the K_M of the GDP-fucose donor substrate. Since our assay conditions far exceed these concentrations, we reasoned our conditions reach enzyme saturation, and we could determine the V_{max} and k_{cat} for FUT8. For the conversion of G0 to G0F, we determined a V_{max} of (0.16 ± 0.01) μM/s, and for the conversion of G0-hexapeptide to G0F-hexapeptide we determined a V_{max} of (0.203 ± 0.006) μM/s. These values correspond to a k_{cat} of (0.53 ± 0.04) s^{-1} when G0 is used as an acceptor, and a k_{cat} of (0.67 ± 0.02) s^{-1} when G0-hexapeptide is used as an acceptor, compared to a k_{cat} of 0.41 s^{-1} for the recombinant FUT8 expressed from *Sf21* cells, which Ihara *et al* (104) had determined using fluorescence-labeled asparagine-linked oligosaccharide as the acceptor. Our results show that there is little difference in substrate preference for the G0 free glycan vs. G0-hexapeptide. This means that the *N*-linkage of the glycan to asparagine is not crucial for FUT8 recognition, and our fluorogenic oligosaccharide substrate MU-G0 can be used as an acceptor for measuring FUT8 activity.

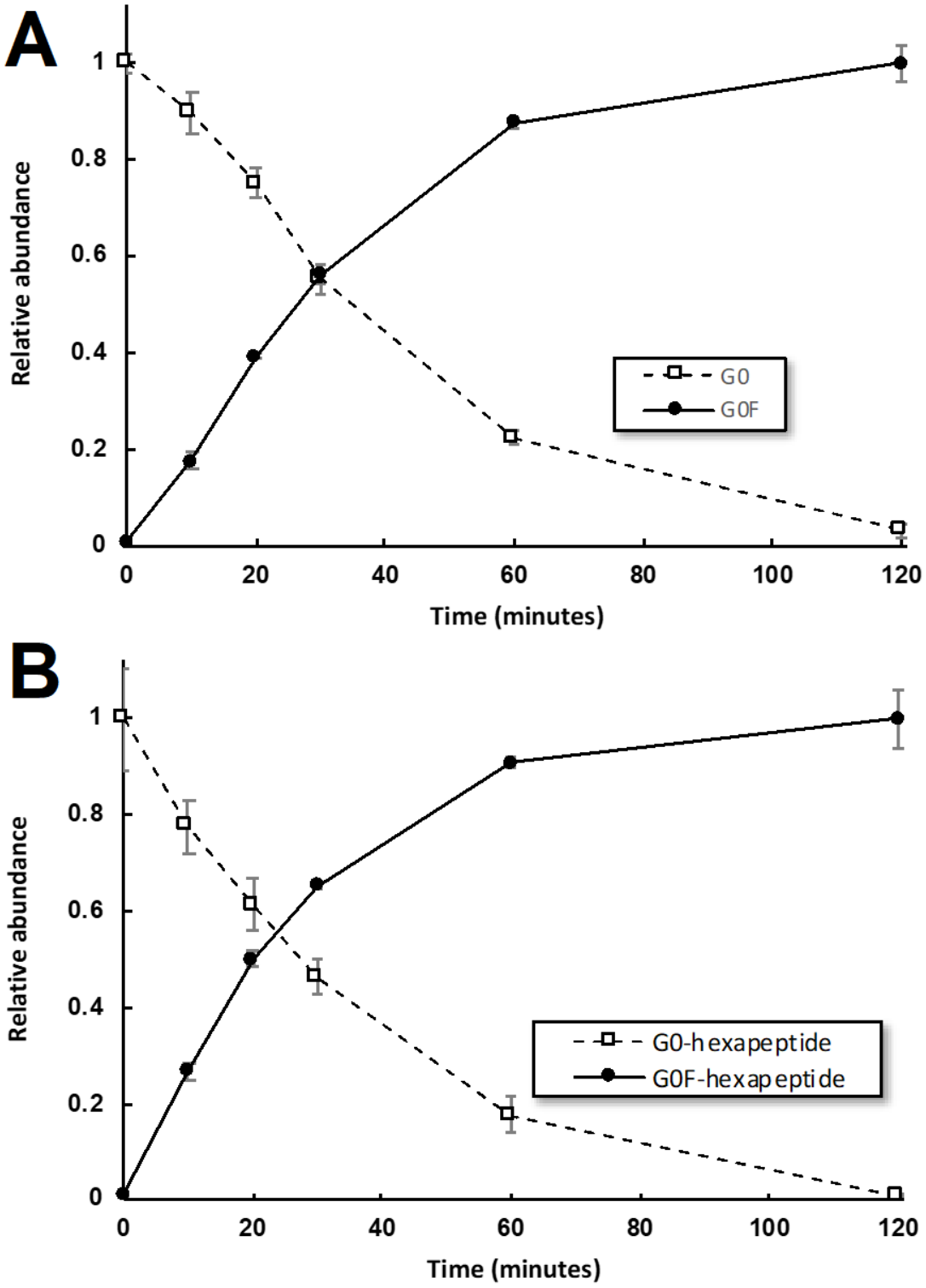

Figure 3.13. FUT8-catalyzed fucosylation of G0 measured by HPLC-MS. (A) HPLC-MS quantitation of 30-minute FUT8 reactions using (37 °C) using G0 (1 µM) as an acceptor and GDP-fucose (10 µM) as a donor with 20 µg/mL of FUT8. (B) HPLC-MS quantitation of 30-minute FUT8 reactions using (37 °C) using G0-hexapeptide (1 µM) as an acceptor and GDP-fucose (10 µM) as a donor with 20 µg/mL of FUT8. Experiments performed in duplicate.

3.3.3 Development and optimization of fluorescence-based assay

In our assay, fucosyltransferase VIII catalyzes the transfer of fucose from GDP-fucose to the synthetic fluorogenic oligosaccharide MU-G0. After a predetermined time, the reaction is heat-inactivated and specific glycosidases are added to the mixture that will sequentially cleave MU-G0 to release the free 4-methylumbelliferone. We expect to see decreased fluorescence in assays with higher FUT8 activity compared to controls where there is none. As was demonstrated above, the *N*-glycosidic linkage to asparagine is unnecessary for substrate recognition by FUT8. However, it remains to be shown experimentally whether FUT8 would recognize the MU-G0 glycan since it bears an *O*-glycosidic bond between the innermost GlcNAc and 4-methylumbelliferyl. Thus, we carried out reactions with 10 μM MU-G0, 100 μM GDP-fucose, and varying amounts of FUT8 in 50 mM sodium phosphate buffered solution. The conversion of MU-G0 to the fucosylated product MU-G0F was observed by mass spectrometry (**Figure 3.14A)**. In 30-minute reactions incubated at 37 °C, the degree of conversion from substrate to product was greater with increasing FUT8 concentration ranging from 0 to 17.5 μg/mL. Furthermore, we also tested whether chitinase from *Streptomyces griseus* (129) could selectively hydrolyze MU-G0 and leave MU-G0F undigested. As such, aliquots of the same FUT8 reaction samples as above were heat-inactivated at 95 °C for 5 minutes and then treated with 0.125 mg/mL of chitinase enzyme for 30 minutes at 37 °C. From HPLC-MS analysis, we observed that the remaining MU-G0 in the samples had been completely hydrolyzed to release 4-methylumbelliferone whereas MU-G0F was left intact (**Figure 3.14B**). The released 4-methylumbelliferone could also be detected by fluorescence measurements and agreed with the results obtained by HPLC-MS detection (**Figure 3.14B**). As was previously demonstrated by Hauser *et al.* (130), our results confirmed that chitinase was able to recognize the *N,N′*-diacetylchitobiose core of a complex-type glycan, cleaving off an *O*-linked 4-methylumbelliferyl group, and that fucosylation of the *N,N′*-diacetylchitobiose moiety abolishes this recognition. We therefore could use this to our advantage in a chitinase-dependent FUT8 activity assay wherein fluorescence signal is inversely proportional to the degree of FUT8-catalyzed fucosylation.

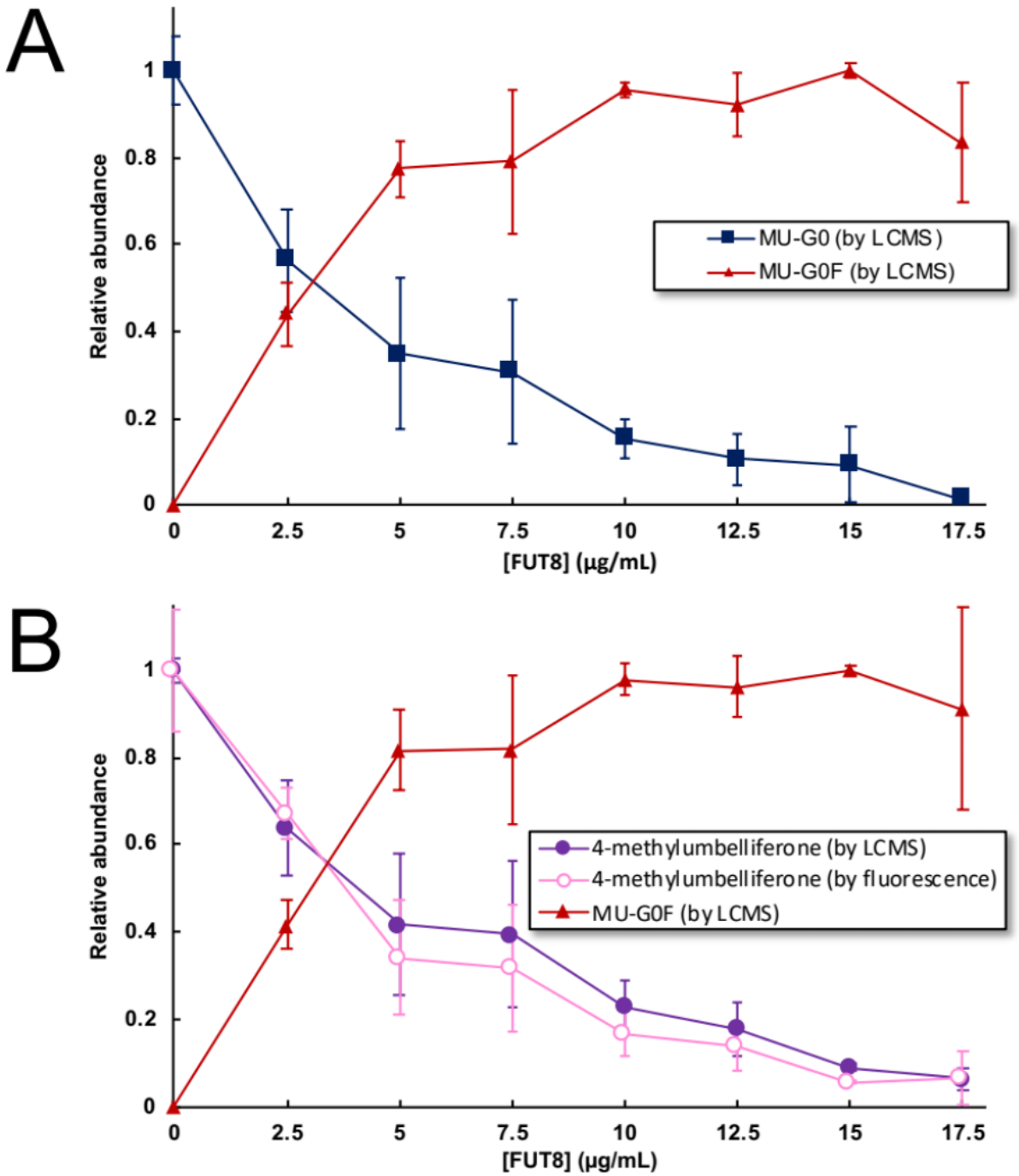

Figure 3.14. FUT8-catalyzed fucosylation of MU-G0 measured by fluorescence or HPLC-MS. (A) HPLC-MS quantitation of 30-minute FUT8 reactions performed (37 °C) using MU-G0 (10 µM) as an acceptor and GDP-fucose (100 µM) as a donor with varying concentrations of FUT8. (B) HPLC-MS and fluorescence quantitation of reactions and free 4-methylumbelliferone following treatment with chitinase. Experiments performed in duplicate.

In further tests, we varied incubation time and donor substrate (GDP-fucose) concentration in our chitinase-dependent FUT8 assay, keeping the MU-G0 acceptor substrate concentration fixed at 10 µM and FUT8 concentration fixed at 8 µg/mL. Assay mixtures contained between 10 to 200 µM of GDP-fucose and were incubated at 37 °C for varying lengths of time before stopping the reactions by heat-inactivation (95 °C for 5 minutes). Once FUT8 was inactivated, fluorescence was developed by adding 0.125 mg/mL chitinase and incubating the mixture to complete digestion at 37 °C for 30 minutes (130). Ideally, the acceptor substrate should be the limiting reagent in our assay and the donor substrate should be in excess to ensure that the reaction reaches as close as possible to completion. We observed that when using only 1 equivalent (10 µM) of GDP-fucose, the FUT8 reaction required more than 3 hours to go to 90 % completion (**Figure 3.15**). In contrast, at the 30-minute mark of the FUT8 reaction, assays containing 40, 100, and 200 µM GDP-fucose had gone to more than 70 %, 80 %, and 90 % completion respectively, whereas the assay containing 10 µM GDP-fucose had gone to about 50 % completion. As such, we chose to use 100 µM GDP-fucose as the optimal concentration of donor substrate.

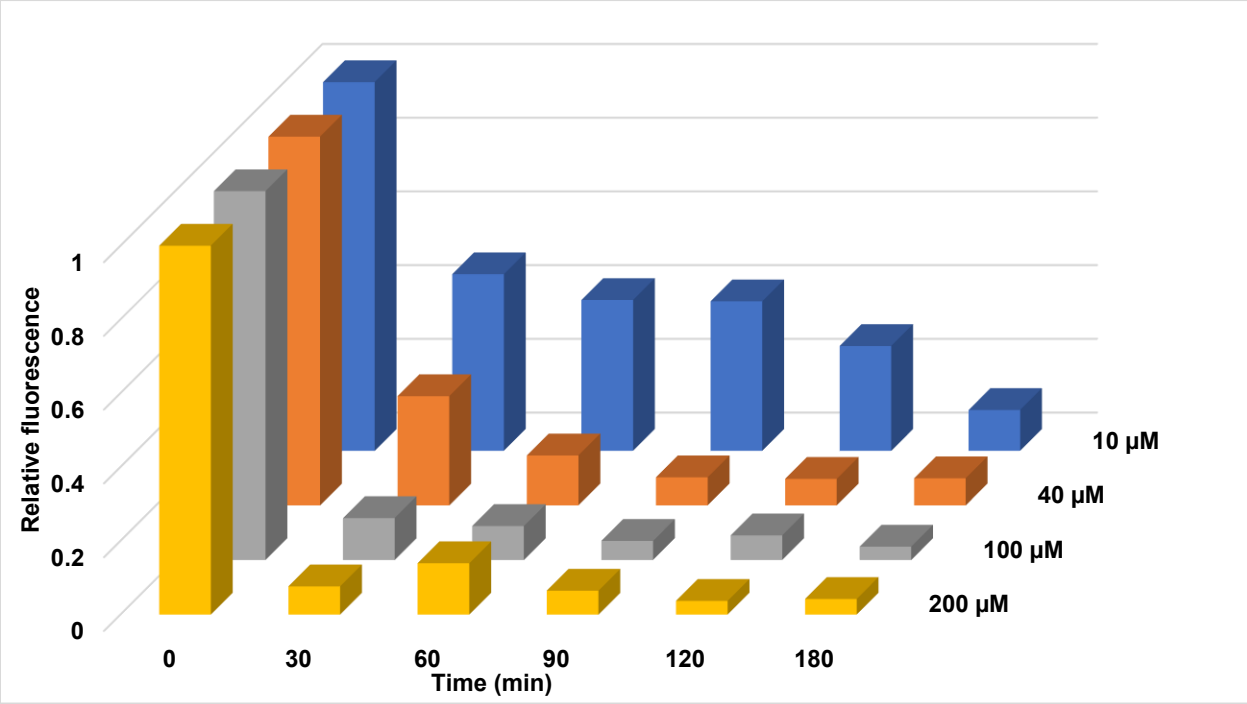

Figure 3.15. Optimization of donor substrate concentration and FUT8 incubation time. FUT8 reactions performed (37 °C) using MU-G0 (10 µM) as an acceptor and varying concentrations of GDP-Fucose as a donor, with 8 µg/mL of FUT8 and 0.125 mg/mL chitinase. Experiments performed in duplicate.

3.3.4 Inhibition of FUT8-catalyzed fucosylation with GDP and GDP-2F-Fuc

Okeley *et al.* (131) reported developing several fucose mimics capable of blocking protein fucosylation in *in vivo* models of cancer. Two of these molecules, 2-fluorofucose and 5-alkynylfucose, were able to effectively shut down the synthesis of fucosylated glycan epitopes and remodel cell-surface carbohydrates. These inhibitors take advantage of the wide substrate specificity of enzymes involved in salvage pathways of fucose synthesis and are converted intracellularly into GDP-fucose analogs. This then leads to a blockage of the de novo pathway of fucose synthesis, resulting in an indirect inhibition of fucosylation, since these fucose analogs cannot be transferred onto cell-surface carbohydrates.

Similarly, Manabe *et al.* (132) developed several GDP-Fucose mimics that displayed inhibitory activity towards FUT8. When using analogs of sugar-nucleotide donor substrates, the high negative charge prevents them from efficiently crossing cell membranes. As such, careful planning is necessary to design non-ionic structures to increase membrane permeability while also maintaining the presence of diphosphates required for binding to FUT8.

While these mimics were demonstrated to be efficient in inhibiting core fucosylation, they lack the specificity and selectivity required to be used as targeted therapeutics in treatments against cancers or other diseases. Thus, the need for small molecule inhibitors against core fucosylation is still prevalent. One benefit of a high-throughput screening assay is the ability to screen large libraries of over 1000 different compounds and identifying several potential inhibitors that could be used as therapeutics. To validate our assay for screening libraries of potential inhibitors, we sought out two previously reported inhibitors of FUT8, namely GDP and GDP-2F-Fucose **(Figure 3.16)**. Our results for the inhibition assay are described below, and also in literature (128).

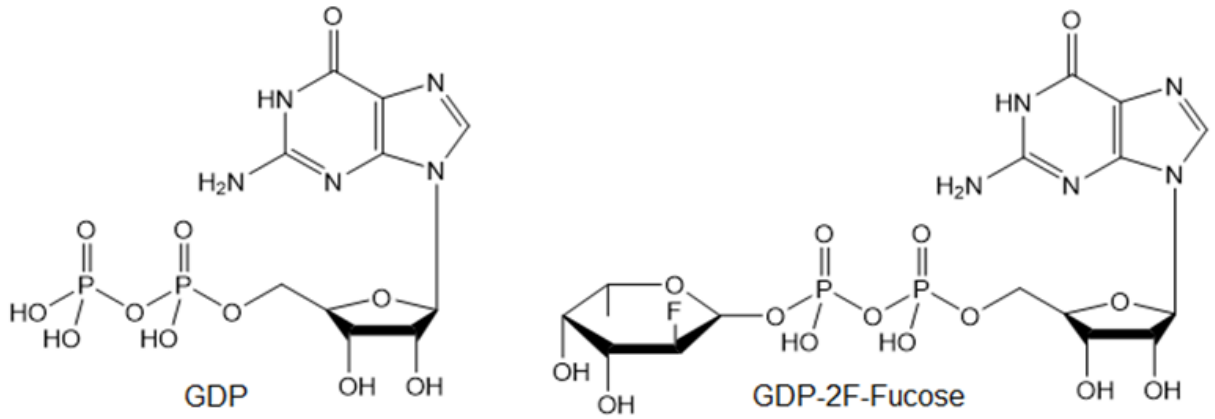

Figure 3.16. Structures of FUT8 inhibitors, GDP and GDP-2F-Fucose.

To assess our assay for detecting inhibition of FUT8, we chose to perform the fucosylation reaction using 8 μg/mL of FUT8, 10 μM of MU-G0 and 100 μM GDP-fucose in 30-minute incubations at 37 °C (prior to heat-inactivation). Under these conditions, in the absence of inhibitor the reaction goes to near-completion, and any significant decrease in activity due to inhibition should produce a measurable difference in the fluorescence signal when incubated with chitinase. Since blockage of fucosylation leads to hydrolysis of MU-G0 by chitinase, inhibition of FUT8 should correspond to an increase in fluorescence intensity compared to controls performed in absence of an inhibitor.

Previously reported fucosyltransferase inhibitors include GDP (104, 131) and guanosine 5′-diphospho-2-deoxy-2-fluoro-β-L-fucose (GDP-2F-Fuc) (131, 133, 134). Using our assay system, we carried out the FUT8 reaction with varying inhibitor concentrations (from 0 to 1 mM of either GDP or GDP-2F-Fuc) and after developing fluorescence with chitinase, we took the intensity of the signal as a measure of FUT8 inhibition. We observed a response curve (**Figure 3.17**) that gave an IC_{50} of 12.9 μM for GDP (consistent with other reports examining GDP as an inhibitor of FUT8 (132)), as demonstrated by the increase in relative fluorescence (because MU-G0 is not being fucosylated which allows chitinase to digest it and release the fluorescent signal). In contrast, we saw no response curve for GDP-2F-Fuc, which suggests it does not directly act as a strong inhibitor of FUT8, although it is known to inhibit FUT3, FUT5, FUT6, and FUT7 (133).

Finally, it is worth noting that our assay system does not distinguish modification of MU-G0 by core fucosylation from any other modification that could also prevent hydrolysis by chitinase. In fact, many FUT8 inhibitors are structural mimics of fucose—often replacing one of the hydroxyl groups by another functionality (133)—and become incorporated into the *N*-glycans of glycoproteins in place of fucose. In this case, our assay strategy may not detect these types of inhibitors as hits but can be of utility if the aim is to screen for inhibitors that prevent core fucosylation without themselves modifying the *N*-glycan.

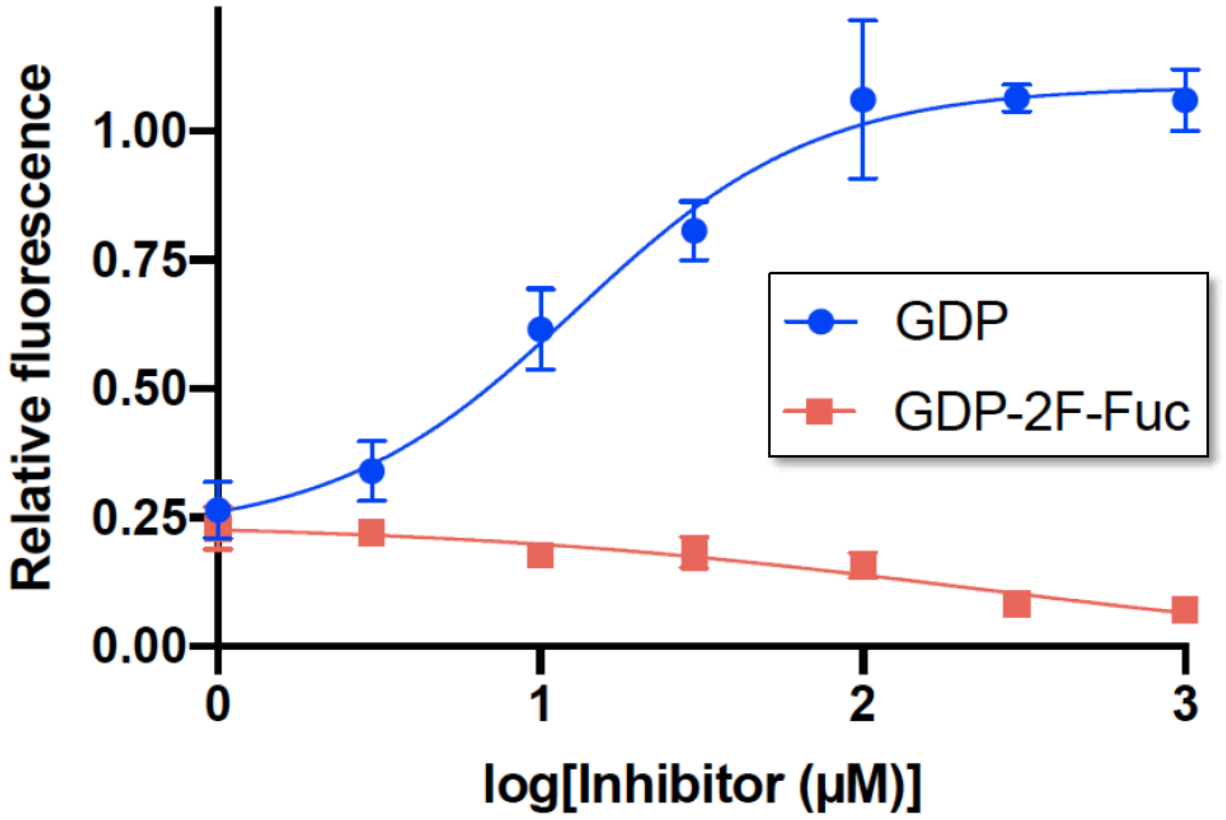

Figure 3.17. Plot of fluorescence signal (indicating inhibition) vs the log of concentration of GDP (blue circles) or GDP-2F-Fuc (red squares). Increase in relative fluorescence indicates inhibition of FUT8 and decrease indicates non-inhibition. Experiments performed in triplicate.

3.3.5 Experimental details for developing the FUT8 activity and inhibition assays

3.3.5.1 Optimizing FUT8 concentration for activity assays

For tests varying FUT8 concentration, different dilutions of FUT8 (0, 5, 15, 20, 25, 30, or 35 µg/ml) were prepared in 10 µl of 50 mM sodium phosphate buffer (pH 7). To these solutions were added 10 µl of 20 mM MU-G0, 200 µM GDP-Fucose in 50 mM sodium phosphate buffer (pH 7) (such that the final concentration of MU-G0 was 10 µM, the final concentration of GDP-fucose was 100 µM, and the concentration of FUT8 varied between 0 and 17.5 µg/mL). The reagents were mixed and incubated for 30 minutes at 37 °C then heat-inactivated at 95 °C for 5 minutes, and the samples were split into two sets. To one set was added 20 µl of 50 mM sodium phosphate buffer (pH 7) as the blank control group. To the other was added 20 µl of 0.25 mg/mL

chitinase in 50 mM sodium phosphate buffer (pH 7). Samples were mixed and fluorescence was measured following incubation for 30 minutes at 37 °C.

3.3.5.2 Optimizing GDP-Fucose concentration and incubation time for activity assays

For further tests varying the concentration of donor substrate and incubation time in the assay system, 100 µl solutions containing 10 µM MU-G0, and varying concentrations of GDP-fucose (10, 40, 100, or 200 µM) and 7.5 µg/ml FUT8 in 50 mM sodium phosphate buffer (pH 7) were prepared and incubated at 37 °C for 3 hours. Aliquots of 10 µl were taken at 0-, 30-, 60-, 90-, 120-, and 180-minute time points and heat-inactivated at 95 °C for 5 minutes. To each sample was added 10 µl of 0.25 mg/mL chitinase in 50mM sodium phosphate buffer (pH 7) and incubated for 30 minutes at 37 °C before measuring fluorescence signals.

3.3.5.3 Synthesis of GDP-2F-Fuc

Synthesis of GDP-2F-Fuc was adapted from the method reported by Rillahan (127). In a 1.5 mL reaction, 5 mg of 2F-Fucose was added with 21.5 mg of ATP and 20.4 mg of GTP to a buffered solution containing 100 mM Tris-HCl (pH 7.5), 20 mM $MgCl_2$, 20 mM $MnCl_2$, and 0.25 mg/ml of FKP. The reaction was left to react at 37°C overnight. The mixture containing GDP-2F-Fuc was then treated with 60 U of alkaline phosphatase (Millipore Sigma, P0114) for an hour at 37 °C to hydrolyze free nucleotides. GDP-2F-Fuc was purified on a Bio-gel P-2 size exclusion column (90 mL resin) eluting with water and fractions containing pure GDP-2F-Fuc were pooled and lyophilized to dry mass, yielding 15 mg (~87 %).

3.3.5.4 Inhibition assay

For testing the inhibition of FUT8, 10 µL solutions with varying concentrations of GDP or GDP-2F-Fuc (0 mM, 0.004 mM, 0.012 mM, 0.04 mM, 0.12 mM, 0.4 mM, 1.2 mM, 4 mM) were prepared in 50 mM sodium phosphate buffer (pH 7) then mixed with 10 µl of 15 µg/ml FUT8, also prepared in 50 mM sodium phosphate buffer (pH 7). The enzyme and inhibitor mixtures were incubated at 37 °C for 10 minutes. Then 20 µl solutions of 20 µM MU-G0 and 20 µl solutions of 200 µM GDP-fucose in 50 mM sodium phosphate buffer (pH 7) were added to the pre-incubated enzyme-inhibitor samples, and the mixtures were incubated at 37 °C for 30 minutes prior to heat-

inactivation at 95 °C for 5 minutes. For fluorescence development, 20 µl aliquots were taken from the samples, and 20 µl of 0.25 mg/mL of chitinase in 50 mM sodium phosphate buffer (pH 7) was added to each. Samples were incubated at 37 °C for 30 minutes before measuring fluorescence. The fluorescence measurements were blank corrected against a control where chitinase was excluded, and then normalized to a control in which FUT8 was excluded.

4 Conclusion

4.1 Summary

Core fucosylation participates in the synthesis of complex glycans that play essential roles in biological processes. The lack of biochemical tools to study core fucosylation makes it particularly difficult to fully understand its mechanisms and functionalities. The purpose of my project was to develop a specific and sensitive assay that can probe the activity and inhibition of FUT8. To achieve our goals, we have performed and validated a well-established extraction procedure for the natural *N*-glycan, sialoglycopeptide, from egg yolk powder. This glycan was used to produce several substrates of FUT8, namely the free glycan G0, the glycopeptide G0-hexapeptide, and the synthetic probe MU-G0. We have described a robust methodology for the production of MU-G0 using a chemo-enzymatic transglycosylation strategy, as well as laid the foundation for an $SnCl_4$-catalyzed chemical glycosylation strategy. We tested our enzymatic assay for the optimal conditions to allow for monitoring the activity of FUT8, as well as demonstrated the capabilities of this assay in identifying potential inhibitors (GDP) and non-inhibitors (GDP-2F-Fuc). We believe that our assay can be used for the high-throughput screening of libraries of small molecule inhibitors and identify potential compounds that can be used as chemotherapeutic agents or for the pharmacological design of ADCC-enhanced antibodies.

References

1. Varki, A., Cummings, R. D. , Aebi, M., Packer, N. H., Seeberger, P. H., Esko, J. D., Stanley, P., Hart, G., Darvill, A., Kinoshita, T., Prestegard, J. J., Schnaar, R. L., Freeze, H. H., Marth, J. D., Bertozzi, C. R., Etzler, M. E., Frank, M., Vliegenthart, J. F., Lütteke, T., Perez, S., Bolton, E., Rudd, P., Paulson, J., Kanehisa, M., Toukach, P., Aoki-Kinoshita, K. F., Dell, A., Narimatsu, H., York, W., Taniguchi, N. & Kornfeld, S. Symbol Nomenclature for Graphical Representations of Glycans. *Glycobiology* **25,** 1323–1324 (2015).
2. Monosaccharidedb.org. (2020). *Monosaccharidedb*. [online] Available at: <http://monosaccharidedb.org/>. [Accessed 27 March 2020].
3. Seeberger, P. H. Monosaccharide Diversity. in (eds. Varki, A. et al.) 19–30 (2015). [online] Available at: <https://www.ncbi.nlm.nih.gov/books/NBK453086/>. [Accessed 27 March 2020].
4. Schnaar, R. L. Glycobiology simplified: diverse roles of glycan recognition in inflammation. *J. Leukoc. Biol.* **99,** 825–838 (2016).
5. Varki, A. Evolutionary forces shaping the Golgi glycosylation machinery: why cell surface glycans are universal to living cells. *Cold Spring Harb. Perspect. Biol.* **3,** (2011).
6. Colley, K. J., Varki, A. & Kinoshita, T. Cellular Organization of Glycosylation. in (eds. Varki, A. et al.) 41–49 (2015). [online] Available at: <https://www.ncbi.nlm.nih.gov/books/NBK453052/>. [Accessed 27 March 2020].
7. Stanley, P., Schachter, H. & Taniguchi, N. N-Glycans. in (eds. Varki, A. et al.) (2009). [online] Available at: <https://www.ncbi.nlm.nih.gov/books/NBK1917/>. [Accessed 24 April 2020].
8. Brockhausen, I., Schachter, H. & Stanley, P. O-GalNAc Glycans. in (eds. Varki, A. et al.) (2009). [online] Available at: <https://www.ncbi.nlm.nih.gov/books/NBK1896/>. [Accessed 24 April 2020].
9. Culyba, E. K., Price, J. L., Hanson, S. R., Dhar, A., Wong, C. H., Gruebele, M., Powers, E. T. & Kelly, J. W. Protein native-state stabilization by placing aromatic side chains in N-glycosylated reverse turns. *Science* **331,** 571–575 (2011).
10. Varki, A. & Gagneux, P. Biological Functions of Glycans. in (eds. Varki, A. et al.) 77–88 (2015). [online] Available at: <https://www.ncbi.nlm.nih.gov/books/NBK453034/>. [Accessed 30 March 2020].

11. Taylor, M. E. & Drickamer, K. Convergent and divergent mechanisms of sugar recognition across kingdoms. *Curr. Opin. Struct. Biol.* **28,** 14–22 (2014).
12. McFarlane, H. E., Doring, A. & Persson, S. The cell biology of cellulose synthesis. *Annu. Rev. Plant Biol.* **65,** 69–94 (2014).
13. Koch, B. E. V, Stougaard, J. & Spaink, H. P. Keeping track of the growing number of biological functions of chitin and its interaction partners in biomedical research. *Glycobiology* **25,** 469–482 (2015).
14. Wassarman, P. M. & Litscher, E. S. Towards the molecular basis of sperm and egg interaction during mammalian fertilization. *Cells. Tissues. Organs* **168,** 36–45 (2001).
15. Kline, K. A., Falker, S., Dahlberg, S., Normark, S. & Henriques-Normark, B. Bacterial adhesins in host-microbe interactions. *Cell Host Microbe* **5,** 580–592 (2009).
16. Rogers, G. N. & Paulson, J. C. Receptor determinants of human and animal influenza virus isolates: differences in receptor specificity of the H3 hemagglutinin based on species of origin. *Virology* **127,** 361–373 (1983).
17. Khatua, B., Bhattacharya, K. & Mandal, C. Sialoglycoproteins adsorbed by Pseudomonas aeruginosa facilitate their survival by impeding neutrophil extracellular trap through siglec-9. *J. Leukoc. Biol.* **91,** 641–655 (2012).
18. Freire-de-Lima, L., Fonseca, L. M., Oeltmann, T., Mendonca-Previato, L. & Previato, J. O. The trans-sialidase, the major Trypanosoma cruzi virulence factor: Three decades of studies. *Glycobiology* **25,** 1142–1149 (2015).
19. Johnston, J. W., Zaleski, A., Allen, S., Mootz, J. M., Armbruster, D., Gibson, B. W., Apicella, M. A. & Munson, R. S. Jr. Regulation of sialic acid transport and catabolism in Haemophilus influenzae. *Mol. Microbiol.* **66,** 26–39 (2007).
20. Cummings, R. D. 'Stuck on sugars - how carbohydrates regulate cell adhesion, recognition, and signaling'. *Glycoconj. J.* **36,** 241–257 (2019).
21. Taylor, M. E., Drickamer, K., Schnaar, R. L., Etzler, M. E. & Varki, A. Discovery and Classification of Glycan-Binding Proteins. in (eds. Varki, A. et al.) 361–372 (2015). [online] Available at: <https://www.ncbi.nlm.nih.gov/books/NBK453061/>. [Accessed 31 March 2020].
22. Gonzalez-Amaro, R. & Sanchez-Madrid, F. Cell adhesion molecules: selectins and integrins. *Crit. Rev. Immunol.* **19,** 389–429 (1999).

23. Akiyama, S. K., Yamada, S. S. & Yamada, K. M. Analysis of the role of glycosylation of the human fibronectin receptor. *J. Biol. Chem.* **264,** 18011–18018 (1989).

24. Zheng, M., Fang, H. & Hakomori, S. Functional role of N-glycosylation in alpha 5 beta 1 integrin receptor. De-N-glycosylation induces dissociation or altered association of alpha 5 and beta 1 subunits and concomitant loss of fibronectin binding activity. *J. Biol. Chem.* **269,** 12325–12331 (1994).

25. Kawano, T., Takasaki, S., Tao, T. W. & Kobata, A. Altered glycosylation of beta 1 integrins associated with reduced adhesiveness to fibronectin and laminin. *Int. J. cancer* **53,** 91–96 (1993).

26. Nadanaka, S., Sato, C., Kitajima, K., Katagiri, K., Irie, S. & Yamagata, T. Occurrence of oligosialic acids on integrin alpha 5 subunit and their involvement in cell adhesion to fibronectin. *J. Biol. Chem.* **276,** 33657–33664 (2001).

27. Ullrich, A., Coussens, L., Hayflick, J. S., Dull, T. J., Gray, A., Tam, A. W., Lee, J., Yarden, Y., Libermann, T. A., Schlessinger, J., Downward, J., Mayes, E. L. V., Whittle, N., Waterfield, M. D. & Seeburg, P. H. Human epidermal growth factor receptor cDNA sequence and aberrant expression of the amplified gene in A431 epidermoid carcinoma cells. *Nature* **309,** 418–425 (1984).

28. Ullrich, A. & Schlessinger, J. Signal transduction by receptors with tyrosine kinase activity. *Cell* **61,** 203–212 (1990).

29. Zhen, Y., Caprioli, R. M. & Staros, J. V. Characterization of glycosylation sites of the epidermal growth factor receptor. *Biochemistry* **42,** 5478–5492 (2003).

30. Tsuda, T., Ikeda, Y. & Taniguchi, N. The Asn-420-linked sugar chain in human epidermal growth factor receptor suppresses ligand-independent spontaneous oligomerization. Possible role of a specific sugar chain in controllable receptor activation. *J. Biol. Chem.* **275,** 21988–21994 (2000).

31. Sun, L., Middleton, D. R., Wantuch, P. L., Ozdilek, A. & Avci, F. Y. Carbohydrates as T-cell antigens with implications in health and disease. *Glycobiology* **26,** 1029–1040 (2016).

32. Zarbock, A., Ley, K., McEver, R. P. & Hidalgo, A. Leukocyte ligands for endothelial selectins: specialized glycoconjugates that mediate rolling and signaling under flow. *Blood* **118,** 6743–6751 (2011).

33. McEver, R. P. Selectins: initiators of leucocyte adhesion and signalling at the vascular wall. *Cardiovasc. Res.* **107,** 331–339 (2015).

34. Somers, W. S., Tang, J., Shaw, G. D. & Camphausen, R. T. Insights into the molecular basis of leukocyte tethering and rolling revealed by structures of P- and E-selectin bound to SLe(X) and PSGL-1. *Cell* **103,** 467–479 (2000).

35. Hanna, S. & Etzioni, A. Leukocyte adhesion deficiencies. *Ann. N. Y. Acad. Sci.* **1250,** 50–55 (2012).

36. Janeway, C. A. & Jr. The structure of a typical antibody molecule. *Immunobiology: The Immune System in Health and Disease. 5th edition.* (1970). [online] Available at: <https://www.ncbi.nlm.nih.gov/books/NBK27144/>. [Accessed: 2 April 2020]

37. Vidarsson, G., Dekkers, G. & Rispens, T. IgG Subclasses and Allotypes: From Structure to Effector Functions. *Frontiers in Immunology* **5,** 520 (2014).

38. Pincetic, A., Bournazos, S., DiLillo, D. J., Maamary, J., Wang, T. T., Dahan, R., Fiebiger, B. M. & Ravetch, J. V. Type I and type II Fc receptors regulate innate and adaptive immunity. *Nat. Immunol.* **15,** 707–716 (2014).

39. Lu, J., Chu, J., Zou, Z., Hamacher, N. B., Rixon, M. W. & Sun, P. D. Structure of FcγRI in complex with Fc reveals the importance of glycan recognition for high-affinity IgG binding. *Proc. Natl. Acad. Sci.* **112,** 833 LP-838 (2015).

40. Anthony, R. M., Kobayashi, T., Wermeling, F. & Ravetch, J. V. Intravenous gammaglobulin suppresses inflammation through a novel T(H)2 pathway. *Nature* **475,** 110–113 (2011).

41. Kaneko, Y., Nimmerjahn, F. & Ravetch, J. V. Anti-inflammatory activity of immunoglobulin G resulting from Fc sialylation. *Science* **313,** 670–673 (2006).

42. Dekkers, G., Plomp, R., Koeleman, C. A., Visser, R., von Horsten, H. H., Sandig, V., Rispens, T., Wuhrer, M. & Vidarsson, G. Multi-level glyco-engineering techniques to generate IgG with defined Fc-glycans. *Sci. Rep.* **6,** 36964 (2016).

43. Hakomori, S. Aberrant glycosylation in cancer cell membranes as focused on glycolipids: overview and perspectives. *Cancer Res.* **45,** 2405–2414 (1985).

44. Kannagi, R. Carbohydrate-mediated cell adhesion involved in hematogenous metastasis of cancer. *Glycoconj. J.* **14,** 577–584 (1997).

45. Kim, Y. J. & Varki, A. Perspectives on the significance of altered glycosylation of glycoproteins in cancer. *Glycoconj. J.* **14,** 569–576 (1997).

46. Fuster, M. M. & Esko, J. D. The sweet and sour of cancer: glycans as novel therapeutic targets. *Nat. Rev. Cancer* **5,** 526–542 (2005).

47. Buckhaults, P., Chen, L., Fregien, N. & Pierce, M. Transcriptional regulation of N-acetylglucosaminyltransferase V by the src oncogene. *J. Biol. Chem.* **272,** 19575–19581 (1997).

48. Schietinger, A., Philip, M., Yoshida, B. A., Azadi, P., Liu, H., Meredith, S. C. & Schreiber, H. A mutant chaperone converts a wild-type protein into a tumor-specific antigen. *Science* **314,** 304–308 (2006).

49. Kakugawa, Y., Wada, T., Yamaguchi, K., Yamanami, H., Ouchi, K., Sato, I. & Miyagi, T. Up-regulation of plasma membrane-associated ganglioside sialidase (Neu3) in human colon cancer and its involvement in apoptosis suppression. *Proc. Natl. Acad. Sci. U. S. A.* **99,** 10718–10723 (2002).

50. Branza-Nichita, N., Negroiu, G., Petrescu, A. J., Garman, E. F., Platt, F. M., Wormald, M. R., Dwek, R. A. & Petrescu, S. M. Mutations at critical N-glycosylation sites reduce tyrosinase activity by altering folding and quality control. *J. Biol. Chem.* **275,** 8169–8175 (2000).

51. Kumamoto, K., Goto, Y., Sekikawa, K., Takenoshita, S., Ishida, N., Kawakita, M. & Kannagi, R. Increased expression of UDP-galactose transporter messenger RNA in human colon cancer tissues and its implication in synthesis of Thomsen-Friedenreich antigen and sialyl Lewis A/X determinants. *Cancer Res.* **61,** 4620–4627 (2001).

52. Kellokumpu, S., Sormunen, R. & Kellokumpu, I. Abnormal glycosylation and altered Golgi structure in colorectal cancer: dependence on intra-Golgi pH. *FEBS Lett.* **516,** 217–224 (2002).

53. Koike, T., Kimura, N., Miyazaki, K., Yabuta, T., Kumamoto, K., Takenoshita, S., Chen, J., Kobayashi, M., Hosokawa, M., Taniguchi, A., Kojima, T., Ishida, N., Kawakita, M., Yamamoto, H., Takematsu, H., Suzuki, A., Kozutsumi, Y. & Kannagi, R. Hypoxia induces adhesion molecules on cancer cells: A missing link between Warburg effect and induction of selectin-ligand carbohydrates. *Proc. Natl. Acad. Sci. U. S. A.* **101,** 8132–8137 (2004).

54. Kalluri, R. & Neilson, E. G. Epithelial-mesenchymal transition and its implications for fibrosis. *J. Clin. Invest.* **112,** 1776–1784 (2003).

55. Nieto, M. A., Huang, R. Y.-J., Jackson, R. A. & Thiery, J. P. EMT: 2016. *Cell* **166,** 21–45 (2016).

56. Thiery, J. P. Epithelial-mesenchymal transitions in tumour progression. *Nat. Rev. Cancer* **2,** 442–454 (2002).

57. Liao, T.-T. & Yang, M.-H. Revisiting epithelial-mesenchymal transition in cancer metastasis: the connection between epithelial plasticity and stemness. *Mol. Oncol.* **11,** 792–804 (2017).

58. Miyoshi, E., Moriwaki, K. & Nakagawa, T. Biological function of fucosylation in cancer biology. *J. Biochem.* **143,** 725–729 (2008).

59. Ma, B., Simala-Grant, J. L. & Taylor, D. E. Fucosylation in prokaryotes and eukaryotes. *Glycobiology* **16,** 158R–184R (2006).

60. Becker, D. J. & Lowe, J. B. Fucose: biosynthesis and biological function in mammals. *Glycobiology* **13,** 41R–53R (2003).

61. Gallatin, W. M., Weissman, I. L. & Butcher, E. C. A cell-surface molecule involved in organ-specific homing of lymphocytes. 1983. *J. Immunol.* **177,** 5–9 (2006).

62. Schneider, M., Al-Shareffi, E. & Haltiwanger, R. S. Biological functions of fucose in mammals. *Glycobiology* **27,** 601–618 (2017).

63. Itai, S., Nishikata, J., Yoneda, T., Ohmori, K., Yamabe, H., Arii, S., Tobe, T. & Kannagi, R. Tissue distribution of 2-3 and 2-6 sialyl Lewis A antigens and significance of the ratio of two antigens for the differential diagnosis of malignant and benign disorders of the digestive tract. *Cancer* **67,** 1576–1587 (1991).

64. Yuan, K., Kucik, D., Singh, R. K., Listinsky, C. M., Listinsky, J. J. & Siegal, G. P. Alterations in human breast cancer adhesion-motility in response to changes in cell surface glycoproteins displaying alpha-L-fucose moieties. *Int. J. Oncol.* **32,** 797–807 (2008).

65. Zhang, Z., Sun, P., Liu, J., Fu, L., Yan, J., Liu, Y., Yu, L., Wang, X. & Yan, Q. Suppression of FUT1/FUT4 expression by siRNA inhibits tumor growth. *Biochim. Biophys. Acta* **1783,** 287–296 (2008).

66. Wang, X., Inoue, S., Gu, J., Miyoshi, E., Noda, K., Li, W., Mizuno-Horikawa, Y., Nakano, M., Asahi, M., Takahashi, M., Uozumi, N., Ihara, S., Lee, S. H., Ikeda, Y., Yamaguchi, Y., Aze, Y., Tomiyama, Y., Fujii, J., Suzuki, K., Kondo, A., Shapiro, S. D., Lopez-Otin, C., Kuwaki, T., Okabe, M., Honke, K. & Taniguchi, N. Dysregulation of TGF-beta1 receptor

activation leads to abnormal lung development and emphysema-like phenotype in core fucose-deficient mice. *Proc. Natl. Acad. Sci. U. S. A.* **102,** 15791–15796 (2005).

67. Fukuda, T., Hashimoto, H., Okayasu, N., Kameyama, A., Onogi, H., Nakagawasai, O., Nakazawa, T., Kurosawa, T., Hao, Y., Isaji, T., Tadano, T., Narimatsu, H., Taniguchi, N., & Gu, J. Alpha1,6-fucosyltransferase-deficient mice exhibit multiple behavioral abnormalities associated with a schizophrenia-like phenotype: importance of the balance between the dopamine and serotonin systems. *J. Biol. Chem.* **286,** 18434–18443 (2011).

68. Wang, X., Gu, J., Ihara, H., Miyoshi, E., Honke, K., & Taniguchi, N. Core fucosylation regulates epidermal growth factor receptor-mediated intracellular signaling. *J. Biol. Chem.* **281,** 2572–2577 (2006).

69. Zhao, Y., Itoh, S., Wang, X., Isaji, T., Miyoshi, E., Kariya, Y., Miyazaki, K., Kawasaki, N., Taniguchi, N., & Gu, J. Deletion of core fucosylation on alpha3beta1 integrin down-regulates its functions. *J. Biol. Chem.* **281,** 38343–38350 (2006).

70. Hashimoto, G., Wright, P. F. & Karzon, D. T. Antibody-dependent cell-mediated cytotoxicity against influenza virus-infected cells. *J. Infect. Dis.* **148,** 785–794 (1983).

71. Shibata-Koyama, M., Iida, S., Okazaki, A., Mori, K., Kitajima-Miyama, K., Saitou, S., Kakita, S., Kanda, Y., Shitara, K., Kato, K., & Satoh, M. The N-linked oligosaccharide at Fc gamma RIIIa Asn-45: an inhibitory element for high Fc gamma RIIIa binding affinity to IgG glycoforms lacking core fucosylation. *Glycobiology* **19,** 126–134 (2009).

72. Shields, R. L., Lai, J., Keck, R., O'Connell, L. Y., Hong, K., Meng, Y. G., Weikert, S. H., & Presta, L. G. Lack of fucose on human IgG1 N-linked oligosaccharide improves binding to human Fcgamma RIII and antibody-dependent cellular toxicity. *J. Biol. Chem.* **277,** 26733–26740 (2002).

73. Ferrara, C., Grau, S., Jäger, C., Sondermann, P., Brünker, P., Waldhauer, I., Hennig, M., Ruf, A., Rufer, A. C., Stihle, M., Umaña, P., & Benz, J. Unique carbohydrate-carbohydrate interactions are required for high affinity binding between FcgammaRIII and antibodies lacking core fucose. *Proc. Natl. Acad. Sci. U. S. A.* **108,** 12669–12674 (2011).

74. Matsumiya, S., Yamaguchi, Y., Saito, J., Nagano, M., Sasakawa, H., Otaki, S., Satoh, M., Shitara, K., & Kato, K. Structural comparison of fucosylated and nonfucosylated Fc fragments of human immunoglobulin G1. *J. Mol. Biol.* **368,** 767–779 (2007).

75. Shinkawa, T., Nakamura, K., Yamane, N., Shoji-Hosaka, E., Kanda, Y., Sakurada, M., Uchida, K., Anazawa, H., Satoh, M., Yamasaki, M., Hanai, N., & Shitara, K. The absence of fucose but not the presence of galactose or bisecting N-acetylglucosamine of human IgG1 complex-type oligosaccharides shows the critical role of enhancing antibody-dependent cellular cytotoxicity. *J. Biol. Chem.* **278,** 3466–3473 (2003).

76. Adamczyk, B., Tharmalingam, T. & Rudd, P. M. Glycans as cancer biomarkers. *Biochim. Biophys. Acta* **1820,** 1347–1353 (2012).

77. Flores, A. & Marrero, J. A. Emerging trends in hepatocellular carcinoma: focus on diagnosis and therapeutics. *Clin. Med. Insights. Oncol.* **8,** 71–76 (2014).

78. Miyoshi, E. & Nakano, M. Fucosylated haptoglobin is a novel marker for pancreatic cancer: detailed analyses of oligosaccharide structures. *Proteomics* **8,** 3257–3262 (2008).

79. Saldova, R., Fan, Y., Fitzpatrick, J. M., Watson, R. W. G. & Rudd, P. M. Core fucosylation and alpha2-3 sialylation in serum N-glycome is significantly increased in prostate cancer comparing to benign prostate hyperplasia. *Glycobiology* **21,** 195–205 (2011).

80. Keeley, T. S., Yang, S. & Lau, E. The Diverse Contributions of Fucose Linkages in Cancer. *Cancers (Basel).* **11,** (2019).

81. Agrawal, P., Fontanals-Cirera, B., Sokolova, E., Jacob, S., Vaiana, C. A., Argibay, D., Davalos, V., McDermott, M., Nayak, S., Darvishian, F., Castillo, M., Ueberheide, B., Osman, I., Fenyö, D., Mahal, L. K., & Hernando, E. A Systems Biology Approach Identifies FUT8 as a Driver of Melanoma Metastasis. *Cancer Cell* **31,** 804–819.e7 (2017).

82. Wang, X., Chen, J., Li, Q. K., Peskoe, S. B., Zhang, B., Choi, C., Platz, E. A., & Zhang, H. Overexpression of alpha (1,6) fucosyltransferase associated with aggressive prostate cancer. *Glycobiology* **24,** 935–944 (2014).

83. Ji, J., Gu, X., Fang, M., Zhao, Y., Yi, C., Wang, A., & Gao, C. Expression of alpha 1,6-fucosyltransferase 8 in hepatitis B virus-related hepatocellular carcinoma influences tumour progression. *Dig. Liver Dis.* **45,** 414–421 (2013).

84. Geng, F., Shi, B. Z., Yuan, Y. F. & Wu, X. Z. The expression of core fucosylated E-cadherin in cancer cells and lung cancer patients: prognostic implications. *Cell Res.* **14,** 423–433 (2004).

85. Tu, C.-F., Wu, M.-Y., Lin, Y.-C., Kannagi, R. & Yang, R.-B. FUT8 promotes breast cancer cell invasiveness by remodeling TGF-beta receptor core fucosylation. *Breast Cancer Res.* **19,** 111 (2017).

86. Liu, Y. C., Yen, H. Y., Chen, C. Y., Chen, C. H., Cheng, P. F., Juan, Y. H., Chen, C. H., Khoo, K. H., Yu, C. J., Yang, P. C., Hsu, T. L., & Wong, C. H. Sialylation and fucosylation of epidermal growth factor receptor suppress its dimerization and activation in lung cancer cells. *Proc. Natl. Acad. Sci. U. S. A.* **108,** 11332–11337 (2011).

87. Ferreira, I. G., Pucci, M., Venturi, G., Malagolini, N., Chiricolo, M., & Dall'Olio, F. Glycosylation as a Main Regulator of Growth and Death Factor Receptors Signaling. *Int. J. Mol. Sci.* **19,** (2018).

88. Zhou, Y., Fukuda, T., Hang, Q., Hou, S., Isaji, T., Kameyama, A., & Gu, J. Inhibition of fucosylation by 2-fluorofucose suppresses human liver cancer HepG2 cell proliferation and migration as well as tumor formation. *Sci. Rep.* **7,** 11563 (2017).

89. Hu, P., Shi, B., Geng, F., Zhang, C., Wu, W., & Wu, X. Z. E-cadherin core fucosylation regulates nuclear beta-catenin accumulation in lung cancer cells. *Glycoconj. J.* **25,** 843–850 (2008).

90. Krapp, S., Mimura, Y., Jefferis, R., Huber, R. & Sondermann, P. Structural analysis of human IgG-Fc glycoforms reveals a correlation between glycosylation and structural integrity. *J. Mol. Biol.* **325,** 979–989 (2003).

91. Yamane-Ohnuki, N. & Satoh, M. Production of therapeutic antibodies with controlled fucosylation. *MAbs* **1,** 230–236 (2009).

92. Beck, A. & Reichert, J. M. Marketing approval of mogamulizumab: a triumph for glyco-engineering. *mAbs* **4,** 419–425 (2012).

93. Illidge, T., Klein, C., Sehn, L. H., Davies, A., Salles, G., & Cartron, G. Obinutuzumab in hematologic malignancies: lessons learned to date. *Cancer Treat. Rev.* **41,** 784–792 (2015).

94. Pereira, N. A., Chan, K. F., Lin, P. C. & Song, Z. The “less-is-more” in therapeutic antibodies: Afucosylated anti-cancer antibodies with enhanced antibody-dependent cellular cytotoxicity. *MAbs* **10,** 693–711 (2018).

95. Videira, P. A., Marcelo, F. & Grewal, R. K. Glycosyltransferase inhibitors: a promising strategy to pave a path from laboratory to therapy. in *Carbohydrate Chemistry: Chemical and Biological Approaches Volume 43* **43,** 135–158 (The Royal Society of Chemistry, 2018).

96. Wilson, J. R., Williams, D. & Schachter, H. The control of glycoprotein synthesis: N-acetylglucosamine linkage to a mannose residue as a signal for the attachment of L-fucose to the asparagine-linked N-acetylglucosamine residue of glycopeptide from alpha1-acid glycoprotein. *Biochem. Biophys. Res. Commun.* **72,** 909–916 (1976).

97. Nakakita, S. i, Menon, K. K., Natsuka, S., Ikenaka, K. & Hase, S. beta1-4Galactosyltransferase activity of mouse brain as revealed by analysis of brain-specific complex-type N-linked sugar chains. *J. Biochem.* **126,** 1161–1169 (1999).

98. Uozumi, N., Yanagidani, S., Miyoshi, E., Ihara, Y., Sakuma, T., Gao, C. X., Teshima, T., Fujii, S., Shiba, T., & Taniguchi, N. Purification and cDNA cloning of porcine brain GDP-L-Fuc:N-acetyl-beta-D-glucosaminide alpha1-->6fucosyltransferase. *J. Biol. Chem.* **271,** 27810–27817 (1996).

99. Yanagidani, S., Uozumi, N., Ihara, Y., Miyoshi, E., Yamaguchi, N., & Taniguchi, N. Purification and cDNA cloning of GDP-L-Fuc:N-acetyl-beta-D-glucosaminide:alpha1-6 fucosyltransferase (alpha1-6 FucT) from human gastric cancer MKN45 cells. *J. Biochem.* **121,** 626–632 (1997).

100. Ihara, H., Ikeda, Y., Toma, S., Wang, X., Suzuki, T., Gu, J., Miyoshi, E., Tsukihara, T., Honke, K., Matsumoto, A., Nakagawa, A., & Taniguchi, N. Crystal structure of mammalian alpha1,6-fucosyltransferase, FUT8. *Glycobiology* **17,** 455–466 (2007).

101. Voynow, J. A., Kaiser, R. S., Scanlin, T. F. & Glick, M. C. Purification and characterization of GDP-L-fucose-N-acetyl beta-D-glucosaminide alpha 1----6fucosyltransferase from cultured human skin fibroblasts. Requirement of a specific biantennary oligosaccharide as substrate. *J. Biol. Chem.* **266,** 21572–21577 (1991).

102. Longmore, G. D. & Schachter, H. Product-identification and substrate-specificity studies of the GDP-L-fucose:2-acetamido-2-deoxy-beta-D-glucoside (FUC goes to Asn-linked GlcNAc) 6-alpha-L-fucosyltransferase in a Golgi-rich fraction from porcine liver. *Carbohydr. Res.* **100,** 365–392 (1982).

103. Staudacher, E. & Marz, L. Strict order of (Fuc to Asn-linked GlcNAc) fucosyltransferases forming core-difucosylated structures. *Glycoconj. J.* **15,** 355–360 (1998).

104. Ihara, H., Ikeda, Y. & Taniguchi, N. Reaction mechanism and substrate specificity for nucleotide sugar of mammalian alpha1,6-fucosyltransferase--a large-scale preparation and characterization of recombinant human FUT8. *Glycobiology* **16,** 333–342 (2006).

105. Kötzler, M. P., Blank, S., Bantleon, F. I., Wienke, M., Spillner, E., & Meyer, B. Donor assists acceptor binding and catalysis of human alpha1,6-fucosyltransferase. *ACS Chem. Biol.* **8,** 1830–1840 (2013).

106. Bertozzi, C. R. & Sasisekharan, R. Glycomics. in (eds. Varki, A. et al.) (2009). [online] Available at: <https://www.ncbi.nlm.nih.gov/books/NBK1965/>. [Accessed: 23 April 2020]

107. Zhang, X., Chen, F., Petrella, A., Chacón-Huete, F., Covone, J., Tsai, T. W., Yu, C. C., Forgione, P., & Kwan, D. H. A High-Throughput Glycosyltransferase Inhibition Assay for Identifying Molecules Targeting Fucosylation in Cancer Cell-Surface Modification. *ACS Chem. Biol.* **14,** 715–724 (2019).

108. Umekawa, M., Li, C., Higashiyama, T., Huang, W., Ashida, H., Yamamoto, K. & Wang, L.-X. (2010) Efficient Glycosynthase Mutant Derived from Mucor hiemalis Endo-β-N-acetylglucosaminidase Capable of Transferring Oligosaccharide from Both Sugar Oxazoline and Natural N-Glycan, *Journal of Biological Chemistry.* **285**, 511-521.

109. Singh, A. K., Pluvinage, B., Higgins, M. A., Dalia, A. B., Woodiga, S. A., Flynn, M., Lloyd, A. R., Weiser, J. N., Stubbs, K. A., Boraston, A. B. & King, S. J. (2014) Unravelling the Multiple Functions of the Architecturally Intricate Streptococcus pneumoniae β-galactosidase, BgaA, *PLOS Pathogens.* **10**, e1004364.

110. Mark, B. L., Vocadlo, D. J., Knapp, S., Triggs-Raine, B. L., Withers, S. G. & James, M. N. G. (2001) Crystallographic Evidence for Substrate-assisted Catalysis in a Bacterial β-Hexosaminidase, *Journal of Biological Chemistry.* **276**, 10330-10337.

111. Wang, W., Hu, T., Frantom, P. A., Zheng, T., Gerwe, B., del Amo, D. S., Garret, S., Seidel, R. D. & Wu, P. (2009) Chemoenzymatic synthesis of GDP-L-fucose and the Lewis X glycan derivatives, *Proceedings of the National Academy of Sciences.* **106**, 16096-16101.

112. Geyer, H. & Geyer, R. Strategies for analysis of glycoprotein glycosylation. *Biochim. Biophys. Acta* **1764,** 1853–1869 (2006).

113. Rich, J. R. & Withers, S. G. Emerging methods for the production of homogeneous human glycoproteins. *Nat. Chem. Biol.* **5,** 206–215 (2009).

114. Kajihara, Y., Suzuki, Y., Yamamoto, N., Sasaki, K., Sakakibara, T., & Juneja, L. R. Prompt chemoenzymatic synthesis of diverse complex-type oligosaccharides and its application to the solid-phase synthesis of a glycopeptide with Asn-linked sialyl-undeca- and asialo-nonasaccharides. *Chemistry* **10,** 971–985 (2004).

115. Verostek, M. F., Lubowski, C. & Trimble, R. B. Selective organic precipitation/extraction of released N-glycans following large-scale enzymatic deglycosylation of glycoproteins. *Anal. Biochem.* **278,** 111–122 (2000).
116. Seko, A., Koketsu, M., Nishizono, M., Enoki, Y., Ibrahim, H. R., Juneja, L. R., Kim, M., & Yamamoto, T. Occurence of a sialylglycopeptide and free sialylglycans in hen's egg yolk. *Biochim. Biophys. Acta* **1335,** 23–32 (1997).
117. Boltje, T. J., Buskas, T. & Boons, G.-J. Opportunities and challenges in synthetic oligosaccharide and glycoconjugate research. *Nat. Chem.* **1,** 611–622 (2009).
118. Liu, L., Prudden, A. R., Bosman, G. P. & Boons, G.-J. Improved isolation and characterization procedure of sialylglycopeptide from egg yolk powder. *Carbohydr. Res.* **452,** 122–128 (2017).
119. Roggentin, P., Rothe, B., Lottspeich, F. & Schauer, R. Cloning and sequencing of a Clostridium perfringens sialidase gene. *FEBS Lett.* **238,** 31–34 (1988).
120. Plummer, T. H. J. & Tarentino, A. L. Purification of the oligosaccharide-cleaving enzymes of Flavobacterium meningosepticum. *Glycobiology* **1,** 257–263 (1991).
121. Kwan, D. H., Ernst, S., Kötzler, M. P. & Withers, S. G. Chemoenzymatic Synthesis of a Type 2 Blood Group A Tetrasaccharide and Development of High-throughput Assays Enables a Platform for Screening Blood Group Antigen-cleaving Enzymes. *Glycobiology* **25,** 806–811 (2015).
122. Kwan, D. H., Constantinescu, I., Chapanian, R., Higgins, M. A., Kötzler, M. P., Samain, E., Boraston, A. B., Kizhakkedathu, J. N., & Withers, S. G. Toward Efficient Enzymes for the Generation of Universal Blood through Structure-Guided Directed Evolution. *J. Am. Chem. Soc.* **137,** 5695–5705 (2015).
123. Huang, G. L. Concise synthesis of 4-methylumbelliferyl-penta-N-acetylchitopentaoside and its inhibition effect on chitinase. *Int. J. Biol. Macromol.* **45,** 381–383 (2009).
124. Umekawa, M., Higashiyama, T., Koga, Y., Tanaka, T., Noguchi, M., Kobayashi, A., Shoda, S., Huang, W., Wang, L. X., Ashida, H., & Yamamoto, K. Efficient transfer of sialo-oligosaccharide onto proteins by combined use of a glycosynthase-like mutant of Mucor hiemalis endoglycosidase and synthetic sialo-complex-type sugar oxazoline. *Biochim. Biophys. Acta* **1800,** 1203–1209 (2010).

125. Noguchi, M., Tanaka, T., Gyakushi, H., Kobayashi, A. & Shoda, S. Efficient synthesis of sugar oxazolines from unprotected N-acetyl-2-amino sugars by using chloroformamidinium reagent in water. *J. Org. Chem.* **74,** 2210–2212 (2009).

126. Gosselin, S., Alhussaini, M., Streiff, M. B., Takabayashi, K. & Palcic, M. M. A continuous spectrophotometric assay for glycosyltransferases. *Anal. Biochem.* **220,** 92–97 (1994).

127. Rillahan, C. D., Brown, S. J., Register, A. C., Rosen, H. & Paulson, J. C. High-throughput screening for inhibitors of sialyl- and fucosyltransferases. *Angew. Chem. Int. Ed. Engl.* **50,** 12534–12537 (2011).

128. Soroko, M. & Kwan, D. H. Enzymatic Synthesis of a Fluorogenic Reporter Substrate and the Development of a High-Throughput Assay for Fucosyltransferase VIII Provide a Toolkit to Probe and Inhibit Core Fucosylation. *Biochemistry* (2020).

129. Mitsutomi, M., Hata, T. & Kuwahara, T. Purification and characterization of novel chitinases from Streptomyces griseus HUT 6037. *J. Ferment. Bioeng.* **80,** 153–158 (1995).

130. Hauser, S., Song, H., Li, H. & Wang, L.-X. A novel fluorescence-based assay for the transglycosylation activity of endo-beta-N-acetylglucosaminidases. *Biochem. Biophys. Res. Commun.* **328,** 580–585 (2005).

131. Okeley, N. M., Alley, S. C., Anderson, M. E., Boursalian, T. E., Burke, P. J., Emmerton, K. M., Jeffrey, S. C., Klussman, K., Law, C. L., Sussman, D., Toki, B. E., Westendorf, L., Zeng, W., Zhang, X., Benjamin, D. R., & Senter, P. D. Development of orally active inhibitors of protein and cellular fucosylation. *Proc. Natl. Acad. Sci. U. S. A.* **110,** 5404–5409 (2013).

132. Manabe, Y., Kasahara, S., Takakura, Y., Yang, X., Takamatsu, S., Kamada, Y., Miyoshi, E., Yoshidome, D., & Fukase, K. Development of alpha1,6-fucosyltransferase inhibitors through the diversity-oriented syntheses of GDP-fucose mimics using the coupling between alkyne and sulfonyl azide. *Bioorg. Med. Chem.* **25,** 2844–2850 (2017).

133. Rillahan, C. D., Antonopoulos, A., Lefort, C. T., Sonon, R., Azadi, P., Ley, K., Dell, A., Haslam, S. M., & Paulson, J. C. Global metabolic inhibitors of sialyl- and fucosyltransferases remodel the glycome. *Nat. Chem. Biol.* **8,** 661 (2012).

134. Burkart, M. D., Vincent, S. P., Düffels, A., Murray, B. W., Ley, S. V., & Wong, C. H. Chemo-enzymatic synthesis of fluorinated sugar nucleotide: useful mechanistic probes for glycosyltransferases. *Bioorg. Med. Chem.* **8,** 1937–1946 (2000).